2

Biochemical and Biomechanical Aspects of Blood Flow

M. Thiriet

REO team
Laboratoire Jacques-Louis Lions, UMR CNRS 7598,
Université Pierre et Marie Curie, F-75252 Paris cedex 05, and
INRIA, BP 105, F-78153 Le Chesnay Cedex.

Abstract. The blood vital functions are adaptative and strongly regulated. The various processes associated with the flowing blood involve multiple space and time scales. Biochemical and biomechanical aspects of the human blood circulation are indeed strongly coupled. The functioning of the heart, the transduction of mechanical stresses applied by the flowing blood on the endothelial and smooth muscle cells of the vessel wall, gives examples of the links between biochemistry and biomechanics in the physiology of the cardiovascular system and its regulation. The remodeling of the vessel of any site of the vasculature (blood vessels, heart) when the blood pressure increases, the angiogenesis, which occurs in tumors or which shunts a stenosed artery, illustrates pathophysiological processes. Moreover, focal wall pathologies, with the dysfunction of its biochemical machinery, such as lumen dilations (aneurisms) or narrowings (stenoses), are stress-dependent. This review is aimed at emphasizing the multidisciplinary aspects of investigations of multiple aspects of the blood flow.

2.1 Introduction

Biomechanics investigates the cardiovascular system by means of mechanical laws and principles. Biomechanical research related to the blood circulation is involved

1. In the motion of human beings, such as gait (blood supply, venous return in transiently compressed veins)
2. In organ rheology influenced by blood perfusion
3. In heat and mass transfer, especially in the context of mini-invasive therapy of tumors
4. Cell and tissue engineering
5. In the design of surgical repair and implantable medical devices

Macroscale biomechanical model of the cardiovascular system have been carried out with multiple goals:

1. Prediction
2. Development of pedagogical and medical tools
3. Computations of quantities inaccessible to measurements
4. Control
5. Optimization

In addition, macroscale simulations deal with subject-specific geometries, because of a high between-subject variability in anatomy, whatever the image-based approaches, either numerical and experimental methods, using stereolithography. The research indeed aims at developing computer-assisted medical and surgical tools in order to learn, to explore, to plan, to guide, and to train to perform the tasks during interventional medicine and mini-invasive surgery. However, this last topic is beyond the goal of the present review.

More and more studies deal with multiscale modeling in order to appropriately take into account the functioning of the blood circulation, from the molecular level (nanoscopic scale, nm), to the cell organelles associated with the biochemical machinery (microscopic scale, μm), to the whole cell connected to the adjoining cells and the extracellular medium, subdomain of the investigated tissue (mesoscopic scale, mm), and to the entire organ (macroscopic scale, cm). The genesis and the propagation

of the electrochemical wave is the signal that commands the myocardium contraction, hence the blood propelling by the heart pump. It is characterized by ion motions across specialized membrane carriers. The myocardium contraction itself requires four-times nanomotors, associated with the actin–myosin binding and detachment. The actin and myosin filaments are assembled in contractile sarcomeres within the cardiomyocytes. The latter microscopic elements gather in muscular fibers, acting as a syncytium in the myocardium. The regulation of the vessel lumen caliber and of the wall structure is mediated by the blood flow (endothelial mechanotransduction). The endothelium is, indeed, permanently exposed to biochemical and biomechanical stimuli which are sensed and transduced, leading to responses that involve various pathways. In particular, the endothelium is subjected to hemodynamic forces (pressure, friction) that can vary both in magnitude and in direction during the cardiac cycle. The endothelium adapts to this mechanical environment using short- and long-term mechanisms. Among the quick reactions, it modulates the vasomotor tone by the release of vasoactive compounds. The endothelium actively participates in inflammation and healing. Chronic adaptation leads to wall remodeling and vascular growth, with the formation of functional collaterals and vessel regression.

2.2 Anatomy and Physiology Summary

Anatomy deals with the macroscopic scale and biochemistry with the nanoscopic level. The cardiovascular system is mainly composed of the cardiac pump and a circulatory network. The heart is made up of a couple of synchronized pumps in parallel, composed of two chambers. The left heart propels blood through the systemic circulation and the right heart through the pulmonary circulation.

The cardiovascular system provides adequate blood input to the different body organs, responding to sudden changes in demand of nutrient supplies. For a stroke volume of 80 ml and a cardiac frequency of 70 beats per mn, a blood volume of 5.6 l is propelled per mn. The travel time for oxygen delivery between the heart and the peripheral tissues has a magnitude $\mathcal{O}(\mathrm{s})$.

2.2.1 Heart

The heart is located within the mediastinum, usually behind and slightly to the left of the sternum (possible mirror-image configuration). The base

of the heart is formed by vessels and atria, and the apex by the ventricles. The septum separates the left and right hearts. The left ventricle is the largest chamber and has the thickest wall. The pericardium surrounds the heart and the roots of the great blood vessels. The pericardium restricts excessive heart dilation, and thus limits the ventricular filling.

Four valves at the exit of each heart cavity, between the atria and the ventricules, the atrioventricular valves, and between the ventricules and the efferent arteries, the ventriculoarterial valves, regulate the blood flow through the heart and allow bulk unidirectional motion through the closed vascular circuit. The tricuspid valve, composed of three cusps, regulates blood flow between the right atrium and ventricle. The pulmonary valve controls the blood flow from the right ventricle into the pulmonary arteries, which carry the blood to the lungs to pick up oxygen. The mitral valve, which consists of two soft thin cups, lets oxygen-rich blood from pulmonary veins pass from the left atrium to the left ventricle. The aortic valve guards the exit of the left ventricle. Like the pulmonary valve, it consists of three semilunar cusps. Immediately downstream from the aortic orifice, the wall of the aorta root bulges to form the Valsalva sinuses. Papillary muscles protrude into both ventricular lumina and point toward the atrioventricular valves. They are connected to chordae tendineae, which are attached to the leaflets of the respective valve.

The heart is perfused by the right and left coronary arteries, originating from the aorta just above the aortic valve. These distribution coronary arteries lie on the outer layer of the heart wall. These superficial arteries branch into smaller arteries that dive into the wall. The heart is innervated by both components of the autonomic nervous system. The parasympathetic innervation originates in the cardiac inhibitory center and is conveyed to the heart by way of the vagus nerve. The sympathetic innervation comes from the cardiac accelerating center. Normally, the parasympathetic innervation represents the dominant neural influence on the heart.

Deoxygenated blood from the head and the upper body and from the lower limbs and the lower torso is brought to the right atrium by the superior (SVC) and by the inferior (IVC) venae cavae. When the pulmonary valves are open, the left ventricle ejects blood into the pulmonary artery. The pulmonary veins carry oxygen-rich blood from the lungs to the left atrium. The aorta receives blood ejected from the left ventricle. The right and left hearts, with their serial chambers, play the role of a lock between a low-pressure circulation and a high-pressure circuit. The atrioventricular and ventriculoarterial couplings set the ventricle for the filling and pressure adaptation and for the ejection, respectively.

The heart has an average oxygen requirement of 6–8 $\mathrm{ml.min^{-1}}$ per 100 g at rest. Approximately 80% of oxygen consumption is related to its mechanical work (20% for basal metabolism). Myocardial blood flow must provide

EDV	70–130 ml
ESV	20–50 ml
SEV	60–100 ml
f_c	60–80 beats.mn^{-1}, $1 - 1.3$ Hz
q	4–7 l.mn^{-1} (70–120 ml.s^{-1})
Ejection fraction	60–80%

Table 2.1. Physiological quantities at rest in healthy subjects. f_c decreases and then increases with aging; SV decreases with aging ($q \sim 6.5$ l.mn^{-1} at 30 years old and $q \sim 4$ l.mn^{-1} at 70 years old).

this energy demand. The myocardium also uses different substrates for its energy production, mostly fatty acid metabolism, which gives nearly 70% of energy requirements, and glucids.

The cardiac output is the amount of blood that crosses any point in the circulatory system and pumped by each ventricle per unit of time. In a healthy person at rest, CO $\sim$ 5–6 l.mn^{-1}. The cardiac output is determined by multiplying the stroke volume (blood volume pumped by the ventricle during one beat) by the heart rate f_c. The stroke volume is the difference between the end-diastolic volume (EDV) and the end-systolic volume (ESV). Values of physiological quantities at rest in healthy subjects are given in Table. 2.1. Various factors determine the cardiac output. The preload is a stretching force exerted on the myocardium at the end of diastole, imposed by the blood volume. The afterload is the resistance force to contraction. The cardiac index is calculated as the ratio between the blood flow rate q and the body surface area ($2.8 < CI < 4.2$ l.mn^{-1}.m^{-2}).

The stroke volume can be modified by changes in ventricular contractility (Frank–Starling effect) and in velocity of fiber shortening. Increased inotropy augments the ventricular pressure time gradient and therefore the ejection velocity. The left ventricle responds to an increase in arterial pressure by augmenting contractility and hence SV, whereas EDV may return to its original value (Anrep effect). An increase in heart rate creates a positive inotropic state (Bowditch or Treppe effect). Most of the signals that stimulate inotropy induce a rise in Ca^{++} influx.

The total oxygen consumption is subject- and age-dependent (2–10 ml/mn/100g). The heart has the highest arteriovenous O_2 difference. Contraction accounts for at least $\sim$75% of myocardial oxygen consumption (MVO2). The coronary blood flow is equal to $\sim$5% of the cardiac output. Whenever O_2 demand increases, various substances promote coronary vasodilatation: adenosine, K^+, lactate, nitric oxide (NO), and prostaglandins. Oxygen extraction in the capillary bed is more effective during diastole because capillaries, which cross the relaxed myocardium, are not collapsed. During systole, the myocardium contraction hinders the arterial perfusion

(systolic compression) but more or less improves the venous drainage, such as the inferior limb venous return that is enhanced by the contraction of surrounding muscles which compress the valved veins. Activation of sympathetic nerves innervating the coronary arteries causes transient vasoconstriction mediated by α1-adrenoceptors. The brief vasoconstrictor response is followed by vasodilation due to augmented vasodilator production and β1-adrenoceptor activation. Parasympathetic stimulation of the heart induces a slight coronary vasodilation.

In order to fit the body needs, the heart increases its frequency and/or the ejection volume. The afterload is determined by the arterial resistances, mainly controlled by the sympathetic innervation (the higher the resistances and the arterial pressure, the smaller the ejected volume). The preload affects the diastolic filling, and, consequently, the end-diastolic values of the ventricular volume and pressure. The blood circulation is controlled by a set of regulation mechanisms, which involve the central command (the nervous system), the peripheral organs via hormone releases, and the local phenomena (mechanotransduction).

The time scale of the short-term regulation of the circulation is $\mathcal{O}(\text{s}) - \mathcal{O}(\text{mn})$, whereas for the long-term one, it is $\mathcal{O}(\text{h}) - \mathcal{O}(\text{day})$. The short-term control includes several reflexes, which involve the following inputs and outputs: the arterial pressure, the heart rate, the stroke volume, and the peripheral resistance and compliance. So the autonomic nervous system can receive complementary information from the circulation and has several processing routes. Control of the peripheral resistance and compliance is slower than command of the heart period and the stroke volume. There are several types of mechanosensitive receptors in the circulation, such as the baroreceptors.

Delayed mechanisms involve circulating hormones such as catecholamines, endothelins (ET), prostaglandins, NO, angiotensin, and others. Late-adaptive mechanisms are provided by the kidneys, which control the volemia through the Na^+ and water reabsorption under action of the renin–angiotensin–aldosterone system (RAAS). Sympathetic stimulation via β1-receptors, renal artery hypotension, and decreased Na^+ delivery to the distal tubules stimulate the release of renin by the kidney. Renin cleaves angiotensinogen into angiotensin 1. Angiotensin-converting enzyme acts to produce angiotensin 2, which constricts arterioles, thereby raising peripheral resistance and arterial pressure. It also acts on the adrenal cortex to release aldosterone, which increases Na^+ and water retention by the kidneys. Angiotensin 2 stimulates the release of vasopressin (or antidiuretic hormone ADH) from the posterior pituitary, which also increases water retention by the kidneys. Angiotensin 2 favors noradrenalin release from sympathetic nerve endings and inhibits noradrenalin reuptake by nerve endings, hence enhancing the sympathetic function.

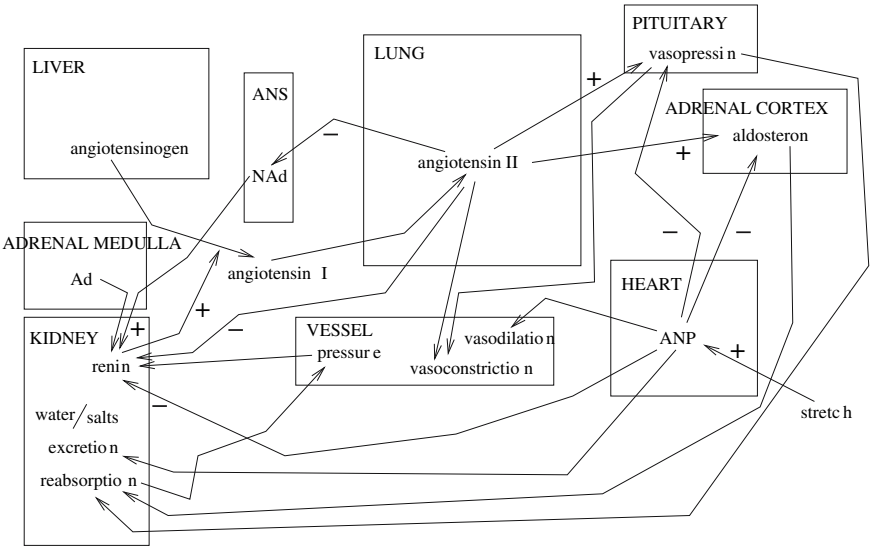

Figure 2.1. The atrial natriuretic peptide (ANP) and the renin–angiotensin system.

The endocrine heart acts as a modulator of the activity of the sympathetic nervous system and the renin–angiotensin–aldosterone system in particular [DEa] (Figure 2.1). The natriuretic peptides control the body fluid homeostasis and the blood volume and pressure. Both ANP (atrial natriuretic peptide or A-type) and BNP (B-type) are synthesized by the cardiac cells as preprohormones, which are processed to yield prohormones and, ultimately, hormones. They then are released into the circulation at a basal rate. Augmented secretion follows hemodynamical or neuroendocrine stimuli. They relax vascular smooth muscle cells and regulate their proliferation. They decrease the baroreflex activity. They inhibit renin release by the kidneys, augment the glomerular filtration rate and decrease the tubular sodium reabsorption. In the adrenal cortex, they inhibit aldosterone synthesis and release.

Cardiac cycle. The heartbeat is a two-stage pumping action over a period of about one second or less: a longer first diastole and a systole. More precisely, the heart rhythm focuses on the activity of the left venticle which consists of four main phases:

1. Isovolumetric relaxation (IR), with closed atrioventricular and ventriculoarterial valves

2. Ventricular filling (VF), subdivided into rapid and reduced filling phases, with open atrioventricular and closed ventriculoarterial valves

Phase	Cycle Timing	Duration	Starting Event
IC	0–50	50	Mitral valve closure ECG R wave peak
SE	50–300	250	Aortic valve opening
IR	300–400	100	Aortic valve closure
VF	400–800	400	Mitral valve opening

Table 2.2. Duration (ms) of the four main phases of the cardiac (left ventricle) cycle ($f_c = 1,25$ Hz, i.e. 75 beats per mn).

3. Isovolumetric contraction (IC), with closed atrioventricular and ventriculoarterial valves

4. Systolic ejection (SE), subdivided into rapid and slow ejection, with closed atrioventricular and open ventriculoarterial valves

Duration of these four phases of the cardiac cycle is given in Table 2.2.

The systole and the diastole are dynamically related. Systolic contraction provides heart recoil and energy which is stored for active diastolic dilation and aspiration [ROb]. Moreover, heart motion during systole pulls the large blood vessels and surrounding mediastinal tissues which react by elastic recoil. Heart diastolic rebound can participate in ventricular filling.

The heart has chaotic behavior. Its irregular nonperiodic behavior characterizes a pump able to react quickly to any changes of the body environment. The normal heartbeat indeed exhibits complex nonlinear dynamics. At the opposite, stable, periodic cardiac dynamics give a bad prognosis. A decay in random variability over time, which is associated with a weaker form of chaos, is indicative of congestive heart failure [POb]. This feature, positive with respect to the heart function, is a handicap in signal and image processing, ensemble averaging being used to improve the signal-to-noise ratio.

2.2.2 Circulatory System

The blood is propelled under high pressure through a network of branching arteries of decreasing size, arterioles, and capillaries to the tissues where it delivers nutrients and removes catabolites. The blood is collected through merging venules and returns to the heart through veins under lower pressures. Each blood circuit (systemic and pulmonary circulation) is thus composed of three main components, arterial, capillary, and venous. The microcirculation starts with the arterioles ($10 < d < 250$ µm; d: vessel caliber) and ends with the venules.

Blood flows depend on the vasculature architecture and local geometry. The vasculature is characterized as a large between-subject variability in vessel origin, shape, path, and branching. Because the flow dynamics strongly depends on the vessel configuration, subject-specific models are required for improved diagnosis and treatment.

2.2.3 Hemodynamics

Hemodynamics differs at the different length scales of the circulatory circuit. In microcirculation, the non-Newtonian two-phase blood flows at low Reynolds number (Re). In the macrocirculation, the blood, supposed to be Newtonian in normal conditions, unsteadily flows at high Re.

The governing equations of a vessel unsteady flow of an incompressible fluid, of mass density ρ, dynamic viscosity μ, and kinematic viscosity $\nu = \mu/\rho$, which is conveyed with a velocity $\mathbf{v}(\mathbf{x}, t)$ ($\mathbf{x}$: Eulerian position; t: time), are derived from the mass and momentum conservation:

$$\begin{aligned} \nabla \cdot \mathbf{v} &= 0, \\ \rho(\mathbf{v}_t + \mathbf{v} \cdot \nabla)\mathbf{v} &= \mathbf{f} + \nabla \cdot \mathbf{C}, \end{aligned} \tag{2.1}$$

where[1] $\mathbf{v}_t \equiv \partial\mathbf{v}/\partial t$, $\mathbf{f} = -\nabla\Phi$ is the body force density (Φ: potential from which body force per unit volume are derived, which is, most often neglected), and $\mathbf{C}$ the stress tensor. The constitutive equation for an incompressible fluid is: $\mathbf{C} = -p_i'\mathbf{I} + \mathbf{T}$, where $p_i' = p_i + \Phi$ (when Φ is neglected, $p_i' = p_i$), $\mathbf{I}$ is the identity tensor, and $\mathbf{T}$ the extra-stress tensor. When the fluid is Newtonian, the stress tensor is a linear expression of the velocity gradient and the pressure; $\mathbf{T} = 2\mu\mathbf{D}$, where $\mu = \mu(T)$ (T: temperature), and $\mathbf{D} = (\nabla\mathbf{v} + \nabla\mathbf{v}^T)/2$ is the deformation rate tensor. The equation set (2.1) leads to the Navier–Stokes equations:

$$\rho(\mathbf{v}_t + (\mathbf{v} \cdot \nabla)\mathbf{v}) = -\nabla p_i' + \mu\nabla^2\mathbf{v}. \tag{2.2}$$

The formulation of the dimensionless equations depends on the choice of the variable scale. The dimensionless equations exhibit a set of dimensionless parameters. The Reynolds number $Re = V_q R/\nu$ (V_q: cross-sectional average velocity; R: vessel radius) is the ratio between convective inertia and viscous effects. When the flow depends on the time, both mean $\overline{Re} = Re(\overline{V_q})$ and peak Reynolds numbers $\widehat{Re} = Re(\widehat{V_q})$, proportional to mean and peak V_q, respectively, can be calculated. $Re = V_q\delta_S/R$ is used for flow stability study (δ_S: Stokes boundary layer thickness). The Stokes

[1] $\nabla = (\partial/\partial x_1, \partial/\partial x_2, \partial/\partial x_3)$, $\nabla\cdot$, and $\nabla^2 = \sum_{i=1}^{3} \partial^2/\partial x_i^2$ are the gradient, divergence, and Laplace operators, respectively.

number $Sto = R(\omega/\nu)^{1/2} = R/\delta_S$ is the square root of the ratio between time inertia and viscous effects. The Strouhal number $St = \omega R/V_q$ is the ratio between time inertia and convective inertia ($St = Sto^2/Re$). The Dean number $De = (R_h/R_c)^{1/2}Re$, for laminar flow in curved vessels, is the product of the square root of the vessel curvature ratio by the Reynolds number. The modulation rate, or amplitude ratio, also plays a role in flow behavior.

The vasculature is made of successive bends and branchings. The embranchment can be, at a first approximation, supposed to be constituted of two juxtaposed bends, with a slip condition on the common wall within the stem. Bends present either gentle or strong curvature, and various curvature angles up to 180 degrees (aortic arch, intracranial segment of the internal carotid artery). The bend then represents the simplest basic unit of the circulatory system. Vessel curvature leads to helical blood motion. The vasculature does not present any symmetric planar bifurcation or junction. Bends, embranchments, and junctions induce 3-D developing flows [THb, THc]. Change in cross-section along the vessel length also generates 3-D flows. Several features affect the flow stability: the vessel curvature according to disturbance amplitude, the wall distensibility, the flow period, and the frequency content of the pressure signal. Laminar flow in blood vessel is a weak assumption.

The mechanical energy provided by the myocardium is converted into kinetic and potential energy associated with the elastic artery distensibility, as well as viscous dissipation. The aortic flow is a discontinuous flow characterized by a strong windkessel effect, with restitution of systolic-stored blood volume during diastole. In the arterial tree, the flow is pulsatile with a possible bidirectional flow period during the cardiac cycle, and back flow in certain arteries, such as in the femoral artery, whereas the flow rate is always positive in other, as in the common carotid artery.

2.2.4 Lymphatics

The circulatory system has a specialized open circuit conveying the lymph into the veins. The lymphatic vessels maintain the fluid balance and are involved in immunity. The lymph has a composition similar to plasma but with small protein concentration. The lymph flow is very slow.

Terminal lymphatics are composed of an endothelium with intercellular gaps surrounded by a highly permeable basement membrane. Larger lymphatic vessels have SMCs and are similar to veins, with thinner walls. Large lymphatic vessels have muscular walls. Lymphatic vessels have valves that prevent back lymph motion. The lymph is thus conveyed into the systemic circulation via the thoracic duct and subclavian veins. Spontaneous and stretch-activated vasomotion in terminal lymphatic vessels helps to convey lymph. Sympathetic nerves cause contraction.

2.2.5 Microcirculation

The microcirculation, with its four main duct components, arterioles, capillaries, venules, and terminal lymphatic vessels, regulates blood flow distribution within the organs, the transcapillary exchanges, and the removal of cell wastes. Arterioles are small precapillary resistance vessels. They are richly innervated by sympathetic adrenergic fibers and highly responsive to sympathetic vasoconstriction via both $\alpha 1$ and $\alpha 2$ postjunctional receptors. Venules are collecting vessels. Sympathetic innervation of larger venules can alter venular tone which plays a role in regulating capillary hydrostatic pressure.

The arteriolar flow is characterized not only by the important pressure loss but also by a decrease in inertia forces and an increase in viscous effects. Both the Reynolds number Re and the Stokes number Sto become much smaller than one. Centrifugal forces do not significantly affect the flow in the microcirculation, where the motion is quasi-independent of the vessel geometry. A two-phase flow appears in the arterioles of a few tens of μm with a near-wall lubrification zone, or plasma layer, and a cell-seeded core. The arteriolar flow is characterized by the Fahraeus effect. The decrease in local Ht associated with the vessel bore can be explained by a selection between the two phases of the blood, the plasma flowing more quickly than the blood cells. The Fahraeus–Lindqvist effect is related to the relative apparent blood viscosity dependence on the tube diameter and hematocrit in small pipes. The Fahraeus–Lindqvist effect can be explained by the interaction of the concentrated suspension of deformable erythrocytes with the vessel wall [FAa].

In the capillaries, the lumen size is smaller than the deformed flowing cell dimension and the plasma is trapped between the cells. The blood flow is then multiphasic. This vasculature compartment does not allow blood phase separation. The blood effective viscosity thus increases in capillaries with respect to its value in arterioles and venules. In this exchange region, where the blood velocity is low, the quantity of interest is the transit time of conveyed molecules and cells. The capillary circulation, characterized by (1) a low flow velocity and (2) a short distance between the capillary lumen and the tissue cells, is adapted to the molecule exchanges.

Fenestrated capillaries have a higher permeability than continuous capillaries. The solvant transport due to the transmural pressure drop Δp is decreased by the difference in osmotic pressures $\Delta\Pi$ due to the presence of macromolecules in the capillary lumen that do not cross the wall. In most capillaries, there is a net filtration of fluid by the capillary endothelium (filtration exceeds reabsorption). A fraction of filtrated plasma is sucked back from the interstitial liquid into capillaries and the remaining part is drained by lymphatic circulation into the large veins. During inflammation,

capillaries become leaky. VEGF, histamine, and thrombin disturb the endothelial barrier [RAa]. In most microvessels, the macromolecule transport is done by transcytosis and not through porous clefts. In microvessels with continuous endothelium, the main route for water and small solutes is the endothelium cleft. The estimated between-cell exchange area is of the order of 0.4% of the total capillary surface area. Transcapillary water flows and microvasculature transfer of solutes, from electrolytes to proteins, in both continuous and fenestrated endothelium, can be described in terms of these porous in-parallel routes.

1. A water pathway across the endothelial cells
2. A set of small pores (caliber of 4–5 nm)
3. A population of larger pores (bore of 20–30 nm) [MIa]

The fiber matrix model of the endothelium glycocalyx and the cleft entrance, associated with pore theory, of capillary permeability sieves solutes [WEa].

2.3 Blood

The blood performs several major functions:

1. Transport through the body
2. Regulation of bulk equilibria
3. Body immune defense against foreign bodies

The blood contains living cells and plasma. The plasma represents approximately 55% of the blood volume. The remaining is hematocrit (Ht), i.e. percent of packed cells. The electrolytes, cations, and anions, contribute to the osmotic pressure Π, which is mainly regulated by the kidneys. Plasma contains 92% water and 8% proteins and other substances. Glucids are energy sources. The fibrinogen acts on platelet and erythrocyte aggregation. Plasma proteins are composed of fibrinogen, albumin, and globulins. They participate in the blood colloidal osmotic pressure which keeps fluids within the vascular system. As does fibrinogen, globulins induce reversible erythrocyte aggregation. The four main types of circulating lipoproteins, which differ in size, density, and content, include chylomicrons, very-low-density lipoproteins (VLDL), low-density lipoproteins (LDL), and high-density lipoproteins (HDL). The lipoproteins convey

cholesterol esters and triglycerides in blood. Triglycerides are delivered to muscles and adipose tissues for energy production and storage. Cholesterol is used to build cell membranes and is a precursor for the synthesis of the steroid hormones, vitamin D, and bile acids. A part is excreted in the biliary ducts as free cholesterol or as bile acids (partial cyclic travel) and another part is conveyed in blood. The lipoproteins are associated with apolipoproteins.

2.3.1 Blood Cells

There are three main kinds of flowing cells: erythrocytes, leukocytes, and platelets (Table 2.3).

Erythrocytes. The erythrocyte or red blood cell (RBC) is a hemoglobin solution bounded by a thin flexible membrane (nonnucleated cell). In its undeformed state, it has a biconcave disc shape with a greater thickness in its outer ring (diameter of 7.7 ± 0.7 μm, central and peripheral thicknesses of 1.4 ± 0.5 μm and 2.8 ± 0.5 μm). It is then susceptible to deformation, in particular with a parachute shape, when moving through tiny capillaries. The RBC shape represents an equilibrium configuration that minimizes the curvature energy of a closed surface for given surface area and volume with a geometrical asymmetry, the phospholipid outer layer of the RBC membrane having slightly more molecules than the inner one. Each RBC contains hemoglobin molecules, which consist of four globin chains α and β. The hemoglobin contains four iron atoms Fe^{2+}, in the center of hemes. It carries oxygen O_2 from lungs to tissues and helps to transport carbon dioxide CO_2 from tissues to lungs. The hemoglobin is also involved in pH regulation. *Reticulocytes* are slightly immature cells (0.5–2% of the total RBC count).

Leukocytes. The leukocyte or white blood cell (WBC) plays a role in immune defense. Five kinds of WBCs exist, three types of *granulocytes*, which have about the same size (8–15 μm), neutrophils, eosinophils, and basophils, and two kinds of agranular leukocytes, lymphocytes (8–15 μm)

Blood Cells	Quantity (mm^{-3})	Cell Volume(%)
RBC	5.10^6	97
WBC	5.10^3	2
thrombocyte	3.10^5	1

Table 2.3. Blood cell approximated geometry and relative concentration.

and monocytes (15–25 μm). The neutrophil is able to phagocytize foreign cells, toxins, and viruses. Scouting neutrophils look for possible invading agents. The eosinophil phagocytizes antigen–antibody complexes. The basophils release two mediator kinds, either from preformed granules or newly generated mediators. The lymphocyte plays an important role in immune response. There are *T-lymphocyte* subsets, inflammatory T cells that recruit macrophages and neutrophils to the site of tissue damage (CD4 + T-cell), cytotoxic T lymphocytes (CTL or CD8 + T-cell) that kill infected, allograft, and tumor cells, and helper T-cells that enhance the production of antibodies by B-cells. The B-lymphocyte produces antibodies. A small fraction of the circulating lymphocytes are natural killer (NK) cells. The monocytes leave the blood stream by diapedesis to become macrophages.

Thrombocytes. Thrombocytes, or platelets, of size 2–4 μm, are cell fragments involved in coagulation. Platelet activation is affected by hemodynamic forces. The two major secretory granule types include numerous α-granules and large dense granules. They contain substances involved in clotting, cell adhesion, and chemotaxis.

Hematopoiesis. All blood cell types are produced in the bone marrow from stem cells. Survival and proliferation are regulated by cytokines and hormones. Many kinds of hematopoeitins ensure a dynamical balance between cell differentiation and proliferation. Erythropoietin, produced by the kidney cortex stimulated by hypoxemia in the renal arteries and by the liver, activates the production of RBCs. The erythropoietin also prevents the destruction of viable tissue surrounding injuries, such as infarction. Thrombopoietin participates in hematopoiesis in general, and to thrombopoiesis in particular. Colony stimulating factors (CSF) stimulate the proliferation of stem cells of the bone marrow in adults. Granulocyte–monocyte colony-stimulating factor (GM-CSF) induces proliferation of multilineage progenitors and the growth of certain WBC colonies. Granulocyte colony-stimulating factor (G-CSF) stimulates proliferation and maturation of monopotent neutrophil progenitors which differentiate into neutrophils. Triggered by macrophage colony-stimulating factors (M-CSF) the granulocyte–macrophage progenitor cells differentiate into monocytes. Stem cell factor (SCF) promotes the production of NK cells. Interleukins (IL) are also involved in the hematopoiesis.

2.3.1.1 Clotting

In normal vessels, the cardiovascular endothelium prevents clotting, because of the presence at the wetted surface of substances such as thrombomodulin, protein C, lipoprotein-associated coagulation inhibitor, tissue factor pathway inhibitor, protease-nexin, and heparan sulfate. The endothelium

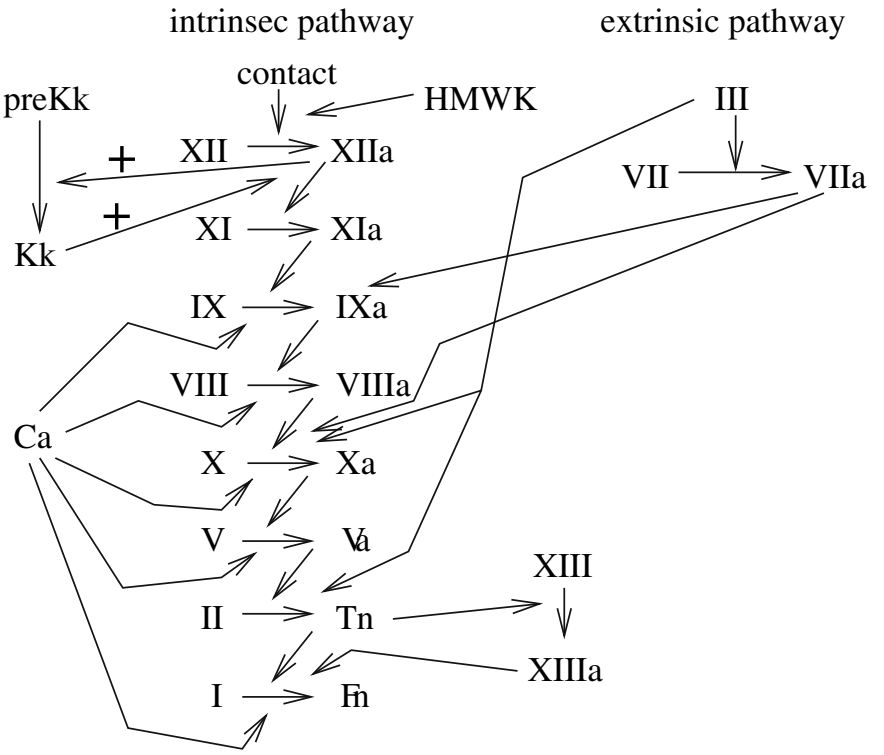

Figure 2.2. Coagulation factors and the reaction cascade. (I: fibrinogen, II: prothrombin, III: tissue thromboplastin, V: proaccelerin, VII: proconvertin, VIII: antihemophilic factor A, IX: antihemophilic factor B, X: Stuart–Prower factor, XI: plasma thromboplastin antecedent, XII: Hageman or contact factor, XIII: fibrin-stabilizing factor, Fn: fibrin, Tn: thrombin, Kk: kallikrein, HMWK: high molecular weight kininogen).

inhibits platelet aggregation by releasing prostacyclins (PGI2) and NO. Figure 2.2.

The endothelium synthesizes coagulation factors, the von Willebrand factor, and tissue factor. When the endothelium is damaged, blood must clot in order to prevent huge bleeding. The hemostatic process depends on the stable adhesion and aggregation of platelets with the subendothelial matrix molecules at the vessel injury site. The primary hemostasis refers to the plug formed by platelets. Various plasma clotting factors form fibrin strands that strengthen the platelet plug. The primary hemostasis involves a set of adhesion receptors and proteins (von Willebrand factor, collagen, fibrinogen, etc.). The secondary hemostasis has two pathways, the intrinsic and the extrinsic one, which join in a common pathway that leads

to fibrin formation. The intrinsic pathway is characterized by the formation of the primary complex on collagen by high-molecular-weight kininogen, prekallikrein, and Hageman factor. The activation cascade transforms fibrinogen into fibrin to form the clot. In the extrinsic pathway, factor VII is activated by the tissue factor to activate factors IX and X. The common pathway begins with activation of factor X by activated factor IX and/or VII. Thrombin is then produced and converts fibrinogen into fibrin. It also activates factors VIII and V as well as platelets.

Mathematical multiscale models of either clotting on a breach of the vessel wall or thrombosis after a rupture of an atherosclerotic plaque have been developed in the presence of a flow of an incompressible viscous fluid [KUa, FOb]. Compounds and platelet transport by convection and diffusion are assumed to take place in a near-wall thin plasma layer. A competition occurs between the activation of the coagulation stages and the removal by the flowing fluid of the clotting factors and cells away from the reaction site. The thrombus growth and embolus shedding from the thrombus can be predicted by the stress field exerted by the moving fluid on the thrombus.

2.3.2 Blood Rheology

The blood can be considered to be a concentrated dispersed RBC suspension in a solution, the plasma, which is composed of ion and macromolecules, especially fibrinogen and globulins, interacting between them and bridging the RBCs. In large blood vessels (macroscale), the ratio between the vessel bore and the cell size ($\kappa_{vp} > \sim 50$) is such that the blood is considered as a continuous homogeneous medium. In capillaries (microscale), $\kappa_{vp} < 1$ and the blood is heterogeneous, transporting deformed cells in a Newtonian plasma. In the mesoscale ($1 < \kappa_{vp} < \sim 50$), the flow is annular diphasic with a core containing cells and a marginal plasma layer.

Shear-step experiments show that the blood has a shear-thinning behavior [CHc]. Blood exhibits creep and stress relaxation during stress formation and relaxation [JOb]. Blood exposures to sinusoidal oscillations of constant amplitude at various frequencies reveal a strain-independent loss modulus and a strain-dependent storage modulus. The blood is a viscoelastic material that experiences a loading history. Furthermore it is thixotropic. Its rheological properties are dictated by the flow-dependent evolution of the blood structural changes, thereby by the kinetics of both RBC aggregation and deformation. The changes in the blood internal structure are indeed due to the reversible RBC aggregation and deformation. The generalized Newtonian model, which is now commonly used when non-Newtonian behavior is considered, is not suitable because it does not take into account the loading history.

The input rheological data, which are provided by experimental results obtained in steady-state conditions, starting from a rouleau network, are far from the physiological ones in the arteries [THd]. In a large blood vessel, the flowing blood is characterized by a smaller convection time scale than the characteristic time of the cell bridging. Therefore, in the absence of stagnant blood regions, the blood, in large vessels, can then be considered to have a constant viscosity. Besides, shear-induced platelet activation has been modeled, using a complex viscoelastic model previously developed [RAc] and a threshold-dependent-triggered activation function [ANa].

2.4 Signaling and Cell Stress-Reacting Components

The cell has a nucleus and several organelles within its cytoplasm, wrapped in a membrane (0.1–10 μm), a phospholipid bilayer with adhesion molecules and other compounds acting in cell junctions in signaling and in substance transport. Biomechanical studies currently deal with larger elements, the cell membrane and the nucleus, as well as the cytoskeleton, which is composed of networks of various types of filaments. The continuum hypothesis is supposed to be valid because the problem length scale, although small with respect to the cell size, remains greater than the cell organelle size. However, the cytoskeleton elements are in general too small. Its behavior is then investigated in a domain that contains a solution of cytoskeleton components rather than the cell itself. The stripped cytoskeleton can also be considered as a discrete structure of stress-bearing components.

2.4.1 Cell Membrane

The plasma membrane, or plasmalemma, is a barrier between the extracellular (ECF) and the intracellular (ICF) fluids. The cell nucleus and organelles have their own membranes. The phospholipid bilayer of the plasma membrane embeds proteins and glucids. The membrane has specialized sites for exchange of information, energy, and nutrients, essentially made from transmembrane proteins.

Phosphoinositides are involved in numerous cell-life events, such as smooth muscle cell contraction and endothelial cell production of vasoactive molecules. Phosphoinositides can specifically interact with proteins having lipid-binding domains. Lipid rafts compartmentalize the membrane into domains, forming microdomains of the cell membrane with phosphoinositides, which are involved in cell endocytosis.

Membrane glucidic copulae of the external membrane layer contribute to the membrane asymmetry. Membrane glucids also participate in the

protein structure and stability of the membrane. Furthermore, membrane glucids modulate the function of membrane proteins. Surface polysaccharides are used directly for cell recognition and adhesion. For example, the laminin, a glycoprotein, allows adhesion of collagen to endothelial cells.

Ion pumps and channels, and gap junctions on the other hand, coordinate the electrical activity and the molecular exchanges. Signal transduction allows the cell to adapt to the changing environment, using various procedures at the molecular scale. The transducers can involve

1. Mechano-sensitive ion channels
2. Conformational changes of molecules
3. Molecular switches in the cell membrane or the cytosol

Many different kinds of receptors, mostly integral membrane proteins, of multiple messengers are localized in the cell membrane. These communication receptors are transduction molecules. Attachment of the ligand on its corresponding receptor induces a reaction cascade. The ligand fixation first triggers synthesis of second messengers, such as cyclic nucleotides, cyclic adenosine monophosphate (cAMP), and cyclic guanosine monophosphate (cGMP), phosphoinositids, and so on, responsible for cell responses of the extracellular ligand (first messenger). Both agonists and antagonists can fix on receptors, generally specific, with or without effect, respectively. Antagonists block agonist fixation. A given messenger can have several receptors. For example, adrenalin has $\alpha 1$, $\alpha 2$, $\beta 1$, and $\beta 2$ receptors, acetylcholine has nicotinic and muscarinic receptors. The receptor types include

1. Receptors coupled to G proteins
2. Receptors whose cytoplasmic domain is activated when the receptor is linked to its ligand and activates one or more specific enzymes to simultaneously stimulate multiple signaling pathways
3. Receptors linked directly or indirectly to ion channels

Protein tyrosine kinases (PTK) modulate multiple cellular events, such as differentiation, growth, metabolism, and apoptosis. PTKs include not only transmembrane receptor tyrosine kinases (RTK) but also cytoplasmic nonreceptor tyrosine kinases (NRTK). Growth factors are major ligands of RTKs. Signaling proteins that bind to the intracellular domain of RTKs include RasGAP, PI3K, phospholipase C γ, phosphotyrosine phosphatase (PTP) SHP, and adaptor proteins involved in the construction of the clathrin coat. The Eph family, the largest family of RTKs, interacts with ephrins. Signaling mediated by ephrins and Eph RTKs regulates a variety of processes including cell shape, cell adhesion and separation, and

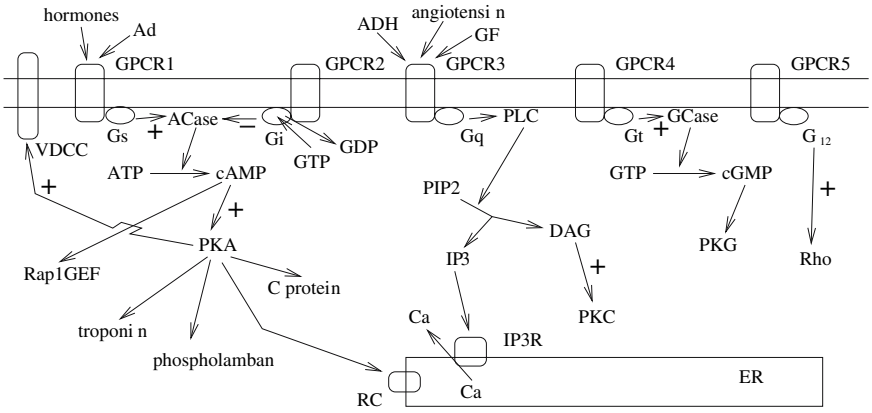

Figure 2.3. G-protein-coupled receptors (GPCR) are associated with G proteins with its three subunits Gα, which binds GDP (inactive state) or GTP, after ligand binding and stimulation, Gβ, and Gγ. Activated Gα activates an effector. Several types of Gα include Gαs (stimulatory), Gαq, Gαi (inhibitory), Gαt, and Gα12. Gαs stimulates adenylyl cyclase (ACase), which produces a second messenger, cyclic AMP (cAMP). Gαq activates phospholipase C (PLC) which generates second messengers, inositol trisphosphate (IP3) and diacylglycerol (DAG). Gαi inhibits adenylyl cyclase. Gαt stimulates guanylyl cyclase (GCase), which forms cyclic GMP (cGMP). Gα12 activates RhoA GTP-binding proteins.

cell motion (attraction and repulsion), modulating the activity of the actin cytoskeleton.

Receptor activation can involve guanosinetriphosphatases (GTPases). These protein switches cycle between two conformations induced by the binding of either guanosine diphosphate (GDP) or guanosine triphosphate (GTP). They then are flicked off (inactive GDP-bound state) and on (active GTP-bound state). The two major kinds of GTPases include the large guanine nucleotide-binding proteins, the G proteins, and the small GTPases.

The G proteins activate (Gs) or inactivate (Gi) adenylate cyclase to regulate the intracellular cAMP level (second messanger) (Figure 2.3). The activation of G proteins is induced by ligand-bound G protein-coupled receptors (GPCR). They then regulate the production or the influx of second messengers. The small Rho GTPases regulate the assembly of filamentous actin (F-actin) in response to signaling. Their effectors induce the assembly of contractile actin–myosin filaments (stress fibers in particular) and of integrin-containing focal adhesions. Thereby, the small Rho GTPases act in vascular processes, such as smooth muscle cell contraction, cell adhesion, endothelial permeability, platelet activation, leukocyte extravasation,

and migration of smooth muscle cells (SMC) and endothelial cells (EC) involved in wall remodeling and angiogenesis [VAa]. They are also required in vascular disorders associated with pathological remodeling and altered cell contractility. The Rho-kinase, an effector of the small Rho GTPase, is involved in atherosclerosis as well as in poststenting restenosis.

Small Rho GTPases can be activated via GPCRs, RTKs, and cytokine receptors. The activation of GTPases into GTP-bound conformations is controlled by specific guanine nucleotide exchange factors (GEF), which activate the Rho GTPases. GTP is hydrolyzed to GDP by the GTPase in combination with GTPase-activating proteins (GAP). In the absence of signaling, the major fraction of small GDP-bound Rho GTPases is sequestrated in the cytosol, bound to guanine dissociation inhibitors (GDI). GDIs slow the rate of GDP dissociation from the Rho GTPases, which remain inactive.

Membrane-associated GTPases Ras and Rho/Rac activate intracellular pathways in response to extracellular signals. The Ras GTPases include Ras, Rap, Ral, and others [BOc]. Both Rap and Ras can bind the same effectors in order to regulate intracellular signaling events. Ras activates effectors, members of the Raf kinase family, the phosphatidylinositol 3 kinase (PI3K) and members of the RalGEF family. Raf activation includes translocation to the plasma membrane, induction of a conformational change by Ras, and phosphorylation. Activated Raf1 activates extracellular signal-regulated kinase (ERK). The Ras-Raf-ERK signal transduction pathway controls proliferation, differentiation, and apoptosis. Cross-actions between the Ras-Raf-ERK and the Ras-Raf-PI3K-protein kinase B (PKB) pathways modulate cell-life modes [ZIa]. ERK belongs to mitogen-activated protein kinases (MAPK), involved in signal transduction. The other main groups of MAPKs include c-Jun N-terminal kinase (JNK) and p38. Mitogen-activated protein kinase p38 is activated by osmotic pressure changes and cytokines. It acts in a cascade that involves the MAPK kinase kinases (MAPKKK) and MAPK kinases (MAPKK) [CHa]. Rho, Rac, and Cdc42 are the three most known classe of the Rho protein family. Each Rho classe has its specific effects on the actin cytoskeleton.

There are many diacylglycerol receptors (DAGR), protein kinase C (PKC) and D (PKD), chimaerins, which target Rho GTPases, and others as translocation activators or inhibitors. PKCδ and PKCϵ are implicated in the evolution of the cardiac function after myocardial infarction [RAd]. PKCδ and PKCϵ are also implicated in vasculogenesis. PKCα and PKCϵ control integrin signaling to ERK [KEb].

Signaling networks are also associated with focal points of enzyme activity. A-kinase anchoring proteins (AKAP) contribute to spatial regulation of signaling events, signal-organizing molecules, targeting protein kinases and phosphatases to specific sites where the enzymes control the

phosphorylation state of neighboring substrates [CAe]. Within a site, a given AKAP can link to diverse substrates. Different AKAPs within a given site can assemble distinct signaling complexes. The displacement of enzymes into and out of these complexes contributes to the temporal regulation of signaling events.

2.4.2 Endocytosis

The endocytosis is the internalization of molecules from the cell surface into membrane compartments, and then into vesicles for cellular trafficking. It starts with the binding between a molecule and its surface receptor. Ligand–receptor interactions often need aggregation of numerous ligand–receptor complexes in a site where the membrane bulges to form a vesicle. The two major paths include clathrin- and caveolae/lipid-raft-mediated endocytosis.

The clathrin-dependent route is responsible for the internalization of nutrients, growth factors, and receptors, as well as antigens and pathogens. Adaptor-proteins stimulate the formation of the clathrin coat. Once inside the cytosol, clathrin is rapidly released for subsequent use by exocytosis (recycling). The naked vesicles fuse with an endosome and the ligands are separated from their receptors. The caveolins form caveolae, types of lipid rafts. The cytoplasmic motion of caveosomes depends on the microtubule network. The caveosome route is regulated by NRTKs and PKC [LEa]. Both clathrin- and caveolae/lipid-raft-mediated endocytosis are modulated by groups of specific kinases. Within each group, some kinases act directly whereas other kinases modulate the endocytic path. Certain kinases exert opposite effects on the two main endocytic kinds for coordination between endocytic routes.

Molecule internalization can also be done by via structures that contain glycosylphosphatidylinositol-anchored proteins (GPI-AP) and fluid-phase markers (caveolae- and clathrin-independent pathway) [KIa]. A transient burst of actin polymerization accompanies endocytic internalization.

2.4.3 Cell Cytoskeleton

The cell deformation and motility is due to the cytoskeleton, a fibril network with articulation nodes from which the cytoskeleton can reorganize itself. In particular, it undergoes stresses and responds to minimize local stresses. The cytoskeleton contracts and forms stiffer bundles to make the cell rigid. Its anchorage on adjacent tissue elements allows an ensemble deformation. Manifold molecules and fibers form this dynamic cell framework which also determines cytosol organization and intracellular displacements [DEb]. There are three classes of cytoskeleton filaments: the

microfilaments, the microtubules, and the intermediary filaments. The spanning network, which fills the whole cytosol, is a fourth element. It can determine the sites of protein synthesis and the assembling locations of filaments and of microtubules. It acts on cell organelle motility.

Microfilaments. The microfilaments contain several proteins. The myosin filaments are localized along the actin filaments. The actin filaments are involved in cell configuration, adhesion, and motility. Actin filaments are anchored on the plasma membrane, using mooring proteins (talin, vinculin) [PAa]. The microfilaments can be used as mooring and transmission lines in a stress field, as towlines during motion. The actin cytoskeleton dynamics is maintained by the balance between actin-binding proteins and actin-severing proteins. Actin aggregation is induced by filamin and cortactin, whereas profilin can inhibit actin polymerization (but stimulates assembly of actin filaments). Cofilin has a depolymerizing activity. α-Actinin favors formation of actin stress fibers.

Microtubules. The microtubules are long polymers of α and β tubulins. The tubulin polymerizes in the presence of guanosine triphosphate and calcium. The microtubule-associated protein facilitates microtubule assembling. The microtubules are thicker and less stable than microfilaments. They are the stiffer element of the cytoskeleton. The microtubules are organized as a scaffolding within the cytoplasm. They control the cell–organelle distribution. Mitochondria and the endoplasmic reticulum (ER) are located along the microtubule network. The microtubules are also necessary for vesicles traveling across the cytosol. Intracellular transport of organelles involves dynein and kinesin. Kinesin is the motor protein for tubulin, which moves along tubulin, as actin does along myosin, having ATPase sites.

The centrosome is a cell body from which the microtubules radiate [GLc]. The centrosome contains two centrioles, each one composed of nine cylindrical elements like a paddle wheel and constituted of three microtubules.

Intermediate filaments. The intermediate filaments cross the cytoplasm either as bundles or isolated elements often in parallel to the microtubules. They are composed of vimentin, desmin, keratin, among others.

Cell motility. The cells display a set of internal motions, change their shape in a stress field, and migrate. Cell motility results from actin polymerization into filaments and depolymerization. The Rho GTPases regulate the actin cytoskeletal dynamics during cell motility and cell shape changes [NOa]. Paxillin (Pax) is a cytoskeletal and focal adhesion docking protein that regulates cell adhesion and migration [TUb]. Pax is also implicated in the regulation of integrin and growth factor signaling. Pax binds to focal adhesion kinase (FAK), vinculin, and interacts with Rho GTPases [SCa].

Modeling of the cytoskeleton mechanics. A 2-D model of the cytoskeleton dynamics has been developed to describe stress-induced interactions between actin filaments and anchoring proteins [CIb]. A small shear induces rearrangment of the four-filament population toward an orientation parallel to the streamwise direction.

Reactive flow model of contractile networks of dissociated cytoplasm under an effective stress in a square domain is associated with a system of non-linear partial derivative equations with boundary conditions [DEd]. Crucial dynamical factors of the cytoskeleton mechanics are

1. The viscosity of the contractile network associated with an automatic gelation as the network density enlarges, without undergoing large deformation

2. A cycle of polymerization-depolymerization

3. A control of network contractibility and of cell-surface adhesion

Tensegrity models consider deformable cells as a set of beams and cables that sustain tension and compression [INa]. The stiffness depends on the prestress level, and for a given prestress state, to the applied stretch, in agreement with experimental findings [WAb].

Extravasation. Circulating blood cells have adhesion receptors that enable the cells subjected to flow forces to adhere to the vessel wall. Flowing cells undergo a sequential-step extravasation, the kinetics of which is shear-dependent. The steps include tethering, rolling, activation, firm adherence, locomotion, diapedesis, and finally transendothelial migration [SCb]. The endothelium can either favor or inhibit flowing cell adhesion on its wetted surface. Adhesion molecules attract the flowing cells toward intercellular spaces for transmigration. Conversely, the endothelium produce 13-hydroxyoctadecadienoic acid (13-HODE) which confers a resistance to platelet or monocyte adherence.

2.4.4 Adhesion Molecules

There are different types of adhesion molecules.

Cadherins. The cadherins, which contain calcium binding sites, connect cells together, one cadherin binding to another in the extracellular space. The cadherin interacts via catenins with actinin and vinculin to link the cadherin–catenin complex to the actin cytoskeleton. Vascular endothelial cadherins (VE-cadherin) anchor the adherens junctions between endothelial cells. p120 Catenin, β-catenin, and α-catenin link VE-cadherin to the actin cytoskeleton.

Selectins. The selectins are expressed in endothelial cells and blood cells for binding two cell surfaces in the presence of Ca^{++}. They slow intravascular leukocytes before transendothelial migration. Three selectin kinds are defined according to the cell in which they were discovered. L-Selectin is expressed on leukocytes for targeting activated endothelial cells. E-Selectin is produced by endothelial cells after cytokine activation. P-Selectin is stored for rapid release in platelet granules or Weibel–Palade bodies of endothelial cells [WAa].

Integrins. The integrins connect actin filaments of the cell cytoskeleton to proteins of the extracellular matrix. Various integrins combine different kinds of two subunits α and β [SMb]. They mediate signaling to or from the environment. They form complexes with cytoskeletal proteins, adaptor proteins, and protein tyrosine kinases, which initiate signaling cascades. They are involved in the regulation of vascular tone and vascular permeability. Various proteins link the integrins to the cytoskeleton, such as tensin and laminin. Among these proteins, certain ones have several binding sites, therefore, cross-linking actin filaments. They include α-actinin, fimbrin, and ezrin-radixin-moesin (ERM).

Ig cell adhesion molecules. Certain members of the immunoglobulin (Ig) superfamily, the Ig cell adhesion molecules (IgCAM), are involved in calcium-independent cell-to-cell binding. Among them, intercellular adhesion molecules (ICAM) are expressed on activated endothelial cells, being the ligand for integrins expressed by WBCs. Platelet–endothelial cell adhesion molecule 1 (PECAM-1) belongs to WBCs, platelets, and intercellular junctions of endothelial cells. Vascular cell adhesion molecule 1 (VCAM-1), once binds to $\alpha_4\beta_1$ integrin, and induces firm adhesion of leukocytes on endothelium.

2.4.5 Intercellular Junctions

Intercellular junctions are tiny specialized regions of the plasma membrane. Several functional categories include

1. Impermeable junctions, which maintain an internal area chemically distinct from surroundings
2. Adhering junctions, which reinforce tissue integrity
3. Communicating junctions for exchange of nutrients and signals with the environment

Within the junctions, membrane proteins have specific configurations. Different histological kinds of intercellular junctions exist.

Desmosomes. The desmosomes contain two classes of desmosomal cadherins, the desmocollins and the desmogleins, each having several subtypes, which are specific to the differentiation status and to the cell type. The intercellular space is filled with filaments that bridge not only membranes but also cytoskeletons of adjacent cells. Two main desmosome types exist. Belt desmosomes contain actin filament susceptible to contract in the presence of ATP, Ca^{++}, and Mg^{++}, in order to close the gap during cell apoptosis. Spot desmosomes contain filaments and transmembrane linkers that connect cytoplasmic networks of tonofilament bundles for mechanical coupling between adjacent cells. Hemidesmosomes allow adhesion of cells to basement membrane. Cells subjected to mechanical stresses have numerous spot desmosomes and hemidesmosomes, which limit cell distensibility and distribute stresses among layer cells and to the underlying tissues to minimize disruptive effects.

Zonula adherens. The zonula adherens is a cell-to-cell adhesion via cadherin–calcium dependent bridging [YAb]. These cadherin-based adhesive contacts link the cytoskeletal proteins of a given cell not only to the cytoskeleton of its neighboring cells, but also to the proteins of the extracellular matrix. Actin filaments are associated with the adherens junctions through catenins.

Tight junctions. Tight junctions leave tiny between-cell space. They selectively modulate paracellular permeability and act as a boundary between the apical and basolateral plasma membranes. Several proteins are involved: cingulin, claudin, occludin, junctional adhesion molecules (JAM), symplekin, zonula occludens proteins (ZO), and so on. E-cadherin is specifically required for tight junction formation and is involved in signaling rather than cell contact [TUa]. The RhoA GTPase regulates the tight-junction assembly and the cell polarity [OZa].

Gap junctions. Gap junctions build between-cell channels, which bridge adjacent membranes. These intercellular protein channels allow low-molecular-weight molecules, small signaling molecules, and ions to diffuse between neighboring cells. Various connexins are involved in gap junctions.

Focal adhesions. Focal adhesions are complexes of clustered integrins and associated proteins that link fibronectin, collagen, laminin, and vitronectin with the cytoskeleton of cultured cells and mediate cell adhesion [ZAb]. Focal adhesion proteins (FAP) include talin, vinculin, tensin, paxillin, and focal adhesion kinase (FAK), among others [CLa]. The focal adhesion kinase mediates several integrin signaling pathways. FAK signaling to Rho GTPases regulates changes in actin and microtubules in cell protrusions of migrating cells.

2.4.6 Extracellular Matrix

The extracellular matrix (ECM) supports cell functions during growth, division, development, differentiation, and apoptosis, as well as tissue formation and remodeling. Cells interact and communicate with other cells and with ECM. ECM is composed of several molecule classes:

1. Structural proteins, collagen, and elastin
2. Specialized proteins, such as fibrillin, laminin, and fibronectin
3. Proteoglycans, or mucopolysaccharides, such as chondroitin sulfate, heparan sulfate, keratan sulfate, and hyaluronic acid

Proteoglycans are composed of a protein to which are attached glycosaminoglycans (GAG). They have an important water-binding capacity, which amplifies the volume occupied by the macromolecules.

Cell anchorage and migration are due to glycoproteins, in particular to fibronectins. These connecting elements are fixed to collagen and elastin of ECM and to the cell membrane on the other hand [HYa]. The fibronectins act on clotting and healing. They also promote chemotaxis [CLb] and activate integrin signaling [GIa].

Proteolytic degradation and remodeling of ECM is controlled by matrix metalloproteinases (MMP) and their inhibitors, the tissue inhibitors of metalloproteinases (TIMP). MMPs are involved in the evolution of atherosclerosis and aneurisms. TIMPs also have mitogenic and cell growth promoting activity.

Basement membrane. The basement membrane (BM) is a specialized extracellular matrix sheet at the interface between the connective tissue and the endothelium. It gives an anchorage surface for endothelium which protects against shearing and detachment. Moreover, it acts as a selective barrier for macromolecular diffusion. It also influences the functions of contacting cells (regulation of cell shape, gene expression, proliferation, migration, and apoptosis) [AUa]. The basement membranes contain laminins, type IV collagen, and proteoglycans. The laminin and type IV collagen networks are linked by nidogens [YUa]. The basement membrane binds a variety of growth factors [GOa].

Interstitial matrix. The interstitial matrix affects the functions of contacting cells. The interstitial matrix has a fibrillar structure, with a large amount of collagen. The structure of the interstitial matrix depends mainly on the type of fibrils and on the type and amount of proteoglycans.

Elastin. A first type of major fibers is given by elastin fibers. The desmosine cross-links elastin to form elastin fibers [ROa]. Elastin binds to cells

via elastonectine. Elastin fibers are the most elastic biomaterials, at least up to a stretch ratio of 1.6 [FUa], the loading and unloading cycles being nearly superimposed. A value of the elastic modulus of elastin fibers of 0.4–0.6 MPa is often considered [AAa, CAd, VIa].

Collagens. The collagens, the second type of major fibers, are structural proteins that form fibrils, characterized by a triplet of helical chains and stabilized by covalent cross-links. The triple helix domain is common for all collagens. The heterogeneity resides in the assembling mode and in the resulting structure. The collagen is surrounded by extensible glycoproteins and proteoglycans. The rheological properties of pure collagen are thus difficult to assess.

The mechanical properties of the blood vessels depend on the interaction between elastic and collagenous elements. Elastin and collagen not only intervene in the vessel wall rheology, via their mechanical properties, their density, and their spatial organization, but also control the function of the smooth muscle cells.

2.4.7 Microrheology

The cell is a complex body that is commonly decomposed into three major rheological components: the plasma membrane, the cytosol, and the viscoelastic nucleus. The membrane and the cytosol can be assumed to be a poroviscoelastic and a poroplastoviscoelastic material, respectively [VEa]. With such a decomposition, macroscopic laws, in particular constitutive laws, are supposed to be valid because the cell size is much greater than the size of its microscopic components.

Rheological sensors must have a suitable size, greater than the size of the cell organelles, as demonstrated by micro- and macrorheometric measurements of the storage and loss moduli [SCc]. Several rheological techniques have been recently developed to explore cell rheology, which include among the usual methods, micropipette technique [EVa], twisting magnetocytometry [LAb], and optical tweezer [HEd]. Micropipette aspiration allows us to study continuous deformation and penetration of a cell into a calibrated micropipette (bore $< 10\ \mu$m) at various suction pressures ($[10^{-1} - 10^{4}$ Pa]) in order to determine a cell's apparent viscosity by measuring the rate of cell deformation and the pressure. The leading edge of the cell is tracked in a microscope to an accuracy of ± 25 nm. Associated basic continuum models, which assume that the cell is a viscous fluid contained in a cortical shell, yield apparent viscosity, shear modulus, and surface tension [YEa]. The results depend on the ratio of the cell size to the micropipette caliber. Soft cells, such as neutrophils and red blood cells, develop about 16 times smaller surface tension than more rigid cells, such as endothelial cells [HOa].

The atomic force microscope (AFM), a combination of the principles of the scanning tunneling microscope and the stylus profilometer, provides a force range of [10pN to 100nN] [BIa]. Twisting magnetocytometry (TMC) uses ligand-coated ferromagnetic beads to apply controlled mechanical stress to cells via specific surface receptors. The sampled cell is subjected to a magnetic field and the bead position is recorded using videomicroscopy. The torque resulting from the shear is measured to determine the viscosity and the elastic modulus using a Kelvin model. The bead size affects the results. Optical tweezers trap dielectric bodies by a focused laser beam through the microscope objective. Optical traps can be used to make quantitative measurements of displacements ($\mathcal{O}(1)$ nm) and forces ($\mathcal{O}(1)$ pN) with time resolution ($\mathcal{O}(1)$ ms).

Measurements have been carried out on round and spread endothelial cells, as well as on isolated nuclei [CAb]. The nonlinear force-deformation curves have been found to be affected by the cell morphology, the nucleus influence being much greater in spread cells, the most common in vivo shape. Cell adhesion affects the cell rheological properties. Due to the cell adaptation to its environment associated with cytoskeleton structural changes, material parameters depend in particular on the cytoskeleton polymerization state (thixotropy). Last but not least, the results of the rheological tests depend not only on the cell state, but also on the techniques, and, for a given technique, on the experimental procedure (cell environment, loading conditions, impacted region size, etc.).

2.5 Heart Wall

The heart wall is composed of several layers:

1. The internal thin endocardium
2. The thick muscular myocardium
3. The external thin epicardium

The double-layered pericardium is composed of the outer parietal pericardium and the epicardium. The pericardial cavity, which contains a lubrificating fluid, separates the two pericardium layers. The heart has a fibrous skeleton with its central fibrous body, which prevents early propagation of action potential. The central fibrous body provides extensions:

1. The valve rings, into which are inserted the cardiac valves
2. The membranous interventricular septum

Mathematical histology. Structure–function features of the heart have been mathematically investigated. Two fiber networks have been particularly studied: the network of collagen fibers of the aortic valve cusp, and the myofibers of the left ventricle wall, using a simple model of mechanically-loaded fibers.

The structure of the aortic leaflet has been derived from its function, which is assumed to consist of supporting a uniform pressure load, undergone by a single family of fibers under tension [PEb]. The equation of equilibrium for the fiber structure is solved to determine its architecture. The computed fiber architecture resembles the real one. Assuming constant myofiber cross-sectional area, symmetry with respect to the ventricle axis, small wall thickness with respect to the other dimensions, and a stress tensor resulting from hydrostatic pressure and myofiber stress, the bundles of myofibers have been shown to be located on approximate geodesics on a nested set of toroidal surfaces centered on a degenerate torus in the equatorial plane of the cylindrical part of the left ventricle [PEa].

Heart valves. The cardiac valves are sheets of connective tissue, attached to the wall at the insertion line. Like the heart wall, the valves are covered by the endothelium. They contain many collagen and elastic fibers and some smooth muscle cells. The cusp is a multilayer structure, with the fibrosa, the spongiosa, and the ventricularis, which is absent in the coaptation region.

In vitro uniaxial traction tests-sort the valve strips in increasing order of stiffness:

1. Axial strips of pulmonary valves
2. Axial strips of aortic valves
3. Circumferential strips of aortic valves
4. Circumferential strips of pulmonary valves [STd]

However, axial and azimuthal strips of porcine aortic valve leaflets are stiffer than the corresponding strips of the pulmonary ones, the circumferential strips being stiffer than the axial ones [JEa].

Heart structure provides the three properties of contractibility, automatism, and conduction due to two kinds of cardiac muscular cells: cardiomyocytes and nodal myocytes.

2.5.1 Cardiomyocyte

Cardiomyocytes (CMC) are striated nucleated cells that are electrically excited in order to contract and relax rhythmically. The striated appearance of the muscle fiber is created by arrays of parallel filaments, the thick

filaments of myosin and the thin filaments of actin. The sarcomere is the anatomical unit of muscular contraction, and the hemisarcomere its functional unit. Myofibrils are held in position by scaffolds of desmin filaments, anchored by costameres enriched in vinculin along the plasma membrane surface. The costameres maintain the spatial structure of sarcomeres and couple CMCs to ECM. The membrane skeleton is made from spectrin and dystrophin, adapting the membrane to CMC functioning and contributing to the force transmission. The costameres, the membrane skeleton, and the cytoskeleton are linked to ECM by membrane protein such as integrins, dystrophin–glycoprotein complexes, and β dystroglycan–laminin bonds. The sarcoplasmic reticulum (SR) broadens out at multiple sites to form junctional SR cisternae tightly coupled to the sarcolemna and its repeated invaginations, the T-tubules. CMCs are joined by intercalated discs which contain gap junctions in order to allow electrochemical impulses, or action potentials, to spread rapidly and orderly so that the cell contraction is almost synchronized.

The contraction is induced by the four-time nanomotor composed of interdigited myosin and actin filaments.

1. The myosin head detaches from actin and fixes ATP.
2. ATP is hydrolized and the myosin head binds to actin.
3. The myosin head releases the phosphate and undergoes a conformational change [RAe].
4. The myosin releases ADP and remains anchored to actin.

CMC interdigitated actin and myosin filaments slide over each other to shorten the sarcomere during contraction (sliding-filament model). The myosin contains myosin heads, which are binding sites for actin and ATP. The troponin and tropomyosin allow actin to interact with myosin heads in the presence of Ca^{++}. When links break, bonds reform farther along actin to repeat the process.

The collagen and elastin fibers form a network forming a surrounding trellis and between-CMC struts, which avoid excessive CMC stretching. Atrial CMCs contain small granules, especially in the right atrium. These granules secrete natriuretic peptides.

Modeling and simulations. Homogenization considers objects of length scale L_o, which have a relative periodicity, and thus are made from repeatable basic units of length scale L_u. In the myocardium, the basic unit contains a limited number of CMCs, inside which the electric field is computed. A constitutive law for the myocardium has been derived from discrete homogenization. A CMC set has been modeled by a quasiperiodic discrete lattice of elastic bars [CAb].

A first stage of heart modeling deals with the mechanical behavior of the myocardium, with its constitutive law. Both systolic and diastolic deformations of the left ventricle are heterogeneous [AZa,FOa,BOa]. Diffusion tensor imaging has been used to characterize cardiac myofiber orientations, with the reduced encoding imaging (REI) methodology [HSa]. The cardiac myofiber direction in each computational mesh element is the mean value of the noisy information contained in the voxels enclosed in the mesh element.

The contraction is more synchronous than the depolarization. The myofibers are differently stretched whether they are early or lately depolarized, without consequences due to their spatial arrangment. Moreover, even if cross-bridging in different cardiomyocytes is simultaneous, the cardiomyocytes can contract differently depending on the force applied to each cardiomyocyte by its own environment. Most of the biomechanical studies have been focused on the mechanical behavior of the left ventricle wall. The material is composite and infiltrated by liquids. Its muscular fibers, with various orientations, are embedded in a matrix with small blood vessels. The myocardial fibers are reinforced and connected by collagen fibers.

The constitutive law takes into account two main phases, active and passive, of the time-dependent heart cyclic behavior. The direct problem computes the stress and strain fields in the given geometry, using given constitutive law and loadings. Finite element models of the left ventricle which undergoes large displacements most often neglect the heterogeneity in wall properties, the myocardial fiber orientation, and the wall thickness variation in the axial and in the azimuthal directions, and assume an uniform transmural pressure. The first simulations were performed in idealized geometries. With the development of medical imaging, imaging data were used to determine the computational domain, reconstructing ventricle cross-section models and, later, heart cavities [HEc]. Numerical results differ from the findings obtained in idealized geometries.

Models of the behavior of the myocardium subjected to large deformations have been developed [ODa]. The Cauchy stress tensor $\mathbf{C}$ is given by $\mathbf{C} = \mathbf{F}(\partial W/\partial \mathbf{G})\mathbf{F}^T - p\mathbf{I}$, where $\mathbf{F}$ is the transformation gradient tensor and $\mathbf{G}$ the Green–Lagrange strain tensor, W the deformation energy function, and p is a Lagrange multiplier. When the material is incompressible, as are most of the biological materials which are rich in water, $det(\mathbf{F}) = 1$. The first Piola–Kirchhoff stress tensor $\mathbf{P}$ is expressed with respect to the deformed configuration: $\mathbf{P} = det(\mathbf{F})\mathbf{F}^{-1}\dot{\mathbf{C}}$. The passive state is defined by the configuration in the absence of internal and external stresses. The active state means myocardium contraction associated with a new configuration but without applied stress (free contraction without environmental constraint). The loaded state corresponds to an active state that undergoes internal and external stresses. The resulting deformation energy function during the cardiac cycle is the sum of three terms, which simulate the

passive ground matrix, the passive elastic, and the active components of the muscular fibers [YAa]. A good agreement is found with experimental data [VIb]. The radial stress is the strain component that has the greatest magnitude during the cardiac cycle. The Cauchy stress reaches its highest value at the beginning of the systolic ejection, between the mid-wall and the endothelium.

In order to derive a constitutive law for the myocardium during the whole cardiac cycle, the heart wall has been modeled by a homogeneous, incompressible, transversally isotropic material [BOd]. The wall behavior during the cardiac cycle is continuously described using several states,

1. A passive unstressed state
2. A virtual state defined by a constant geometry but a rheology change
3. An active state of contraction without rheology change

The time-dependent strain energy function is composed of two terms, a passive and an active strain energy function (SEF) associated with the passive fibers and with the cardiomyocytes, respectively:

$$W(\mathbf{G}, t) = W_{pas}(\mathbf{G}) + \beta(t) W_{act}(\mathbf{G})$$

($\beta(t)$: activation function).

2.5.2 Nodal Cells

Nodal cells are small muscular cells with few myofibrils, which create or quickly spread the depolarization wave in the myocardium. The electrochemical signal starts with the spontaneous depolarization of the nodal cells of the sino-atrial node (SAN), the "natural pacemaker". The action potential spreads through the atria to reach the atrioventricular node (AVN) and to produce atrial contraction. This node imposes a short delay in impulse transmission to the ventricles. The action potential then runs in the His bundle and the Purkinje fibers, which penetrate into the myocardium to end on CMCs.

Ion pumps and exchangers of the CMC membrane maintain steep ion concentration and electrical gradients across the membrane. The resting membrane potential is ~ -88 mV (inside negative). The action potential is initiated by depolarization of the sarcolemna. The Na^+ channels open first and then rapidly inactivate. The quick cellwards Na^+ motion increases the transmembrane potential to $\sim +30$ mV (phase 0). Phase 1 corresponds to the first rapid repolarization associated with a transient outward motion of K^+. Phase 2 is associated with a slow inward Ca^{++} current (plateau), involving L-type Ca^{++} channels. During phase 3, delayed

rectifier K^+ channels induce rapid repolarization. Throughout phase 4, the resting membrane potential is regulated by a background K^+ current. The refractory period is a protective mechanism in order to maintain efficient successive blood fillings and ejections.

2.5.3 Excitation–Contraction Coupling

The intracellular calcium content is an important factor that triggers the contraction, determining the inotropy. Its removal kinetics from the cytosol characterizes the heart lusitropy. Voltage-dependent Ca^{++} channels (VDCC) are located at sarcolemmal–sarcoplasmic reticulum junctions close to the ryanodine channels (Figure 2.4). They induce a Ca^{++} influx and elicit Ca^{++} release from the ryanodine channels with a negative feedback [SIa]. Moreover, the Ca^{++} influx is limited by Ca^{++}-dependent inactivation of the channels due to calmodulin [ZUa]. The protein S100A1 increases Ca^{++} release from the sarcoplasmic reticulum by interacting with ryanodine channels. Ca^{++} release from the sarcoplasmic reticulum into the cytoplasm sufficiently increases the cytosolic $[Ca^{++}]_i$ to induce contraction. $Na^+ - Ca^{++}$ porters, which exchange three Na^+ for one Ca^{++}, operate during phase 2, stabilizing $[Ca^{++}]_i$. Relaxation requires Ca^{++} removal from the cytosol, by sarco(endo)plasmic reticulum Ca^{++}-ATPase (SERCA) pumps, by $Na^+ - Ca^{++}$ exchangers (NCX), by mitochondrial Ca^{++} uniporters, and by plasma membrane Ca^{++}-ATPase pumps (PMCA). Phospholamban, which is associated with SERCA, inhibits this pump. Protein kinase A (PKA) phosphorylates phospholamban, and thus has a lusitropic effect. Most Ca^{++} returns to SR where it is stored by bonds with calsequestrin.

The second stage of heart modeling refers to the genesis and the propagation of the action potential. The epicardial depolarization and deformation of the ventricular wall have been simultaneously measured using electrode brushes and videorecording of optical markers [DEc] or multielectrode socks

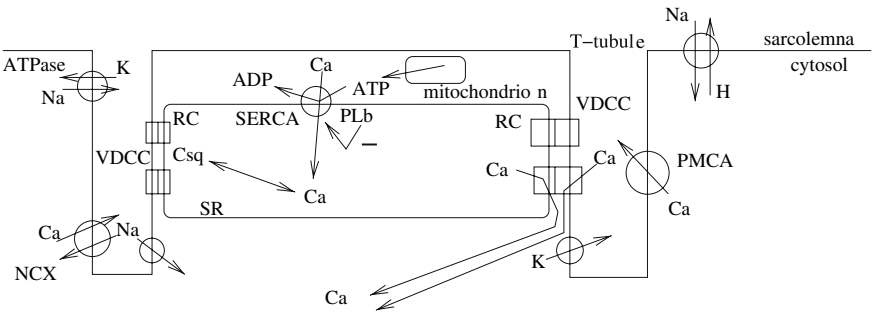

Figure 2.4. The cardiomyocyte, its ion carriers and calcium fluxes.

and MRI tagging [FAb]. The electrochemical wave propagation model provides the arrival time of the depolarization in the various parts of the myocardium, the local myofiber orientations affecting the ventricular depolarization timing due to the anisotropic myocardium conductivity. However, the nodal tissue remains difficult to locate.

The basic tractable phenomenological monodomain model of depolarization and repolarization consists of two variables $\mathtt{u}$ and $\mathtt{v}$ [FIa, Naa], in which fast dynamics are coupled to slow ones. The Aliev–Panfilov model gives an example of dimensionless FitzHugh–Nagumo system [ALa].

Bidomain models have been proposed to simulate electrophysiological waves in the myocardium [GEa, BOe]. Bidomain models take into account the intracellular and the extracellular spaces, separated by the CMC syncytium membrane. Both domains have their own volume-averaged properties, especially the conductivity of the extra- and intracellular spaces. The problem to numerically solve is very complex. Cardiac fibers have anisotropic conduction properties, the impulse propagation being faster in the axial direction than transversally. A conductivity tensor $\mathbf{M}$ is then introduced, assuming that the conductivity values are identical in all directions perpendicular to the muscular fiber direction [COa]. The collection of CMCs, end-to-end or side-to-side connected by specialized junctions, immersed in the extracellular fluid and ground matrix, is modeled as a periodic array that leads to a homogenization procedure, with homogenized conductivity tensors $\mathbf{M}_i$ and $\mathbf{M}_e$. The membrane current density J_m is then given by:

$$J_m = -\nabla \cdot \mathbf{i}_i = \nabla \cdot \mathbf{M}_i \nabla \mathtt{u}_i = \nabla \cdot \mathbf{i}_e = -\nabla \cdot \mathbf{M}_e \nabla \mathtt{u}_e,$$

where $\mathtt{u}_i$ and $\mathtt{u}_e$ are the electric potentials of the intra- and extracellular spaces and $\mathbf{i}_i$ and $\mathbf{i}_e$ the currents $(\nabla \cdot (\mathbf{M}_i \nabla \mathtt{u}_i + \mathbf{M}_e \nabla \mathtt{u}_e) = 0)$. In its general form, the bidomain model is defined by [BOe]:

$$\kappa_{av}(\mathtt{C}_m \mathtt{u}_t + 1/\mathtt{R}_m \, f(\mathtt{u}, \mathtt{v})) = \nabla \cdot (\mathbf{M}_i \nabla \mathtt{u}_i),$$

where $\mathtt{u} = \mathtt{u}_i - \mathtt{u}_e$ is the action potential, $\mathtt{v}$ the recovery variable, κ_{av} the surface area-to-volume ratio of the cardiac myofibers, and $\mathtt{C}_m$ and $\mathtt{R}_m$ the cell membrane capacitance and resistance.

2.5.3.1 Electromechanical Coupling

The electromechanical ICEMA model of the electrochemical wave propagation is based on the FitzHugh–Nagumo equations and the myocardium functioning model on the Hill–Maxwell rheological model, associated with the muscular fiber direction and the dynamics equations [BEb, CHb, SEa]. The ICEMA heart model thus connects the microscopic and macroscopic enumerate levels, via a mesoscopic step. The constitutive equations require

a small number of state variables, so that the solution of direct problems can be quickly obtained and inverse problems can be solved.

The Huxley nanoscopic-scale sliding filament theory states that the binding f and rupture g frequencies of the actin–myosin bridges are functions of the elongation x [HUd]. The cross-bridge proportion n with elongation $\tilde{x} = x/\ell$ (ℓ: maximum bridge length) with the kinetics defined by f and g is given by:

$$\dot{n} = dn/dt = (1-n)f - ng. \tag{5.1}$$

The sarcomere contraction generates a shortening $s = s_0(1+\epsilon_{\mathbf{c}})$ ($\epsilon_{\mathbf{c}}$: sarcomere deformation), with a velocity $s_0\dot{\epsilon}_{\mathbf{c}}$ assuming a synchronized motion of the set of bridgings (subscript c: contractile component). The theory of actin–myosin cross-bridge dynamics and the moments [ZAa] applied to the cross-bridge model describes the contraction at the sarcomere and at the myofiber scale, respectively.

The functioning of the nanomotors, i.e. the actin and myosin molecules, is controlled by Ca^{++} and adenosine triphosphate. $[Ca^{++}]_i$ has been given by a relatively simple function of time [HUc]. The amount of calcium linked to troponin C is commonly assumed to be equal to the cytosolic concentration, i.e. to the extent of the calcium influx driven by the action potential. The myocardium contraction results from a conformational change of the actin–myosin bridge, coupled with ATP hydrolysis. A unique command signal ($\mathtt{u} > 0$ during contraction and $\mathtt{u} < 0$ during active relaxation) has been defined, which involves two parameters, k_{ATP}, mainly the ATP hydrolysis rate, which is regulated by the actin–troponin–tropomyosin complex and k_{Ca}, the calcium extraction rate by the sarcoplasmic reticulum [BEb]. Such a model does not take into account either the oxygen consumption or the link between the ATP and Ca^{++}. Heart mitochondria use more oxygen, but produce ATP at a faster rate than liver ones [CAc]. Ca^{++} overload can induce mitochondrial dysfunction in disease in the presence of a pathological stimulus. Calcium, ATP, and reactive oxygen species (ROS) are indeed in close connection [BRa]. The mitochondrion produces ATP, which synthesis is stimulated by Ca^{++}. The dysregulation of mitochondrial Ca^{++} can lead to elevated concentration of ROS and apoptosis.

The collective behavior of the sarcomere fibers is governed by the relationship between the stress σ and the strain ϵ in the myofiber direction (viscoelastoplastic behavior). The evolution of the stiffness $k_{\mathbf{c}}$ and the active stress $\sigma_{\mathbf{c}}$ of the contractile component, knowing the strain rate $\dot{\epsilon_{\mathbf{c}}}$ and the command $\mathtt{u}$, are given by the following set of ordinary differential equations [BEa].

$$\begin{cases} \dot{k}_{\mathbf{c}} = -(\alpha|\dot{\epsilon}_{\mathbf{c}}| + |\mathtt{u}|)k_{\mathbf{c}} + k_0|\mathtt{u}|_+ \\ \dot{\sigma}_{\mathbf{c}} = k_{\mathbf{c}}\dot{\epsilon}_{\mathbf{c}} - (\alpha|\dot{\epsilon}_{\mathbf{c}}| + |\mathtt{u}|)\sigma_{\mathbf{c}} + \sigma_0|\mathtt{u}|_+ \\ \sigma \;\; = d(\epsilon_{\mathbf{c}})(\sigma_{\mathbf{c}} + k_{\mathbf{c}}\tilde{x}_0) + \mu_{\mathbf{c}}\dot{\epsilon}_{\mathbf{c}} \end{cases}. \tag{5.2}$$

The parameters k_0 and σ_0 are related to the maximum available actin–myosin cross-bridges in the sarcomere. $d(\epsilon_{\mathbf{c}}) \in (0,1)$ is the modulation function of the active stress which accounts for the length-tension curve[2] and $\mu_{\mathbf{c}}$ the viscosity ($k_{\mathbf{c}}(0) = \sigma_{\mathbf{c}}(0) = 0$). The cross-bridge detachment rate is given by $|\mathtt{u}| + \alpha|\dot{\epsilon}_{\mathbf{c}}|$.

The action potential $\mathtt{u}$ is modeled by the two-variable Aliev–Panfilov equation system [ALa]:

$$\begin{cases} \mathtt{u}_t - \nabla \cdot (\kappa_e \nabla \mathtt{u}) = f(\mathtt{u}) - \mathtt{v} \\ v_t = \varepsilon(\beta \mathtt{u} - \mathtt{v}) \end{cases}, \tag{5.3}$$

where $\varepsilon \ll 1$, $f(\mathtt{u}) = \mathtt{u}(\mathtt{u} - \alpha)(\mathtt{u} - 1)$ ($\alpha \in [0, 1/2]$), and κ_e is an electrical conductivity.

In the macroscopic scale, the cardiac fibers are embedded in a collagen sheath, connected by collagen struts and supported by a ground matrix with elastin fibers. The mesoscopic myofiber constitutive law is incorporated in a Hill–Maxwell rheological model [CHb]. The sarcomere set of a myofiber is represented by a single contractile element (CE). The activity of CE depends on the action potential $\mathtt{u}$. The electrochemically driven contraction and relaxation obey Eq. (5.2). The isometric deformations are modeled by an elastic serial element (ESE) in series with CE. ESE lengthens when CE shortens at a constant myofiber length. A third viscoelastic element (EPE) in parallel to the CE-ESE branch is introduced. EPE educes the force developed from a certain myofiber length in the absence of stimulation. These three components are not related to the muscle constituents.

The cardiac tissue is supposed to be not purely incompressible [SAa].

$$\mathbf{P} = -p \det(\mathbf{F}) \mathbf{S}_r^{-1} + \sigma_p^e(\mathbf{G}) + \sigma_p^v(\mathbf{G}, \dot{\mathbf{G}}) + \sigma_{1D}\, \hat{\mathbf{f}} \otimes \hat{\mathbf{f}}, \tag{5.4}$$

where $\mathbf{P}$ denotes the second Piola–Kirchhoff stress tensor, $p = -B(\det(\mathbf{F}) - 1)$ (B: bulk modulus, used as coefficient of incompressibility penalization), $\mathbf{F}$ the deformation gradient, $\mathbf{G}$ the Green–Lagrange strain tensor, and $\mathbf{S}_r$ the right Cauchy–Green deformation tensor, $\sigma_p^e(\mathbf{G}) \propto \rho_0 \partial W^e / \partial \mathbf{G}$ (elastic part of EPE, ρ_0: density of the reference state, W^e: elastic strain energy density), and $\sigma_p^v(\mathbf{G}, \dot{\mathbf{G}}) = \partial W^v / \partial \dot{\mathbf{G}}$ (viscoelastic part of EPE, W^v: viscous strain energy pseudo-density) the stresses in the passive materials, σ_{1D} the stress generated by the active element CE, and $\hat{\mathbf{f}}$ the local unit direction vector of the myofiber.

[2] The troponin C sensitivity for Ca^{++} and the cross-bridge availability depend on the sarcomere length.

In the preliminary stage, the valves are not incorporated in the model. Constraints on the volume variations of the ventricle are then added:

$$\begin{cases} q \geq 0 \text{ when } p_V = p_a & \text{(ejection)} \\ q = 0 \text{ when } p_A < p_V < p_a & \text{(isovolumic phases)} \\ q \leq 0 \text{ when } p_V = p_A & \text{(filling)} \end{cases}, \tag{5.5}$$

where $q = -\dot{V}_V$ is the blood flow ejected from the ventricle (V_V: ventricular volume), p_V the ventricular blood pressure, p_A the atrial pressure, and p_a the arterial pressure. A regularization is used to overcome numerical failures on flow rate computations. A windkessel or a 1-D model of the blood flow provides p_a.

Using Eqs. (5.2) and (5.4), and incorporating the multiple elements of the simplified system

1. The myofibers
2. The passive components
3. The valve model
4. The upstream atrium and the exiting artery

the following equation set is obtained [CHb].

$$\begin{cases} \rho\ddot{\mathbf{u}} - \nabla \cdot (\mathbf{F} \cdot \sigma) = 0 \\ \sigma = \sigma_{1D}\, \hat{\mathbf{f}} \otimes \hat{\mathbf{f}} + E_p(\mathbf{G}) \\ \sigma_{1D} = \sigma_{\mathbf{c}}/(1+\epsilon_s) = \sigma_s/(1+\epsilon_{\mathbf{c}}) \\ \sigma_{\mathbf{c}} = E_{\mathbf{c}}(\epsilon_{\mathbf{c}}, \mathtt{u}) \\ \sigma_s = E_s((\epsilon_{1D} - \epsilon_{\mathbf{c}})/(1+\epsilon_{\mathbf{c}})) \\ \epsilon_{1D} = \sum_{i,j} G_{ij} f_i f_j \\ \dot{\mathtt{g}} = \mathcal{G}(\mathtt{g}, t) \\ \text{initial + boundary conditions} \end{cases}, \tag{5.6}$$

where $E_p(\mathbf{G}) = -p\det(\mathbf{F})\mathbf{S}_r^{-1} + \sigma_p(\mathbf{G}, \dot{\mathbf{G}})$, $E_{\mathbf{c}}$ is a function expressing system (5.2), and ϵ_{1D} is the deformation in the myofiber direction. From thermomechanical considerations, $1 + \epsilon_{1D} = (1+\epsilon_{\mathbf{c}})(1+\epsilon_s)$. $\mathtt{g}$ stands for V_V, or p_V, or p_A, or p_a, the last equation accounting for the set of ordinary differential equations modeling the valve opening and closure and the arterial pressure changes.

The action potential is initiated at the ends of the Purkinje network localized according to the literature data [DUb]. The model parameters

are calibrated according to the available data, which provide

1. The arterial parameters [STb, WEb]
2. $k_{\mathbf{c}}$ and $\tau_{\mathbf{c}}$ [WUa], from which are computed the respective asymptotic values k_0 and σ_0
3. The estimation of the passive behavior from conflicting literature data [VEb, PIb]

2.5.4 Vessel Wall

As blood pulses in an artery, its wall alternatively stretches and rebounds. Wall expansion and relaxation are due to the rheological properties of the vessel wall, and, thus to its composition and structure.

Main structural elements. The structure components exist in every kind of blood vessel, except capillaries, although the element amount and the structure vary between the vessel types. Endothelial cells line the blood–wall interface. The specific cells of connective tissues are fibroblasts, which produce the ground matrix and fibers, and fibrocytes. Elastin provides vessel distensibility and collagen tensile strength. Smooth muscle cells (SMC) are responsible for the lumen size.

Wall structure. The wall structure is circumferentially layered. The tunica number and tunica structure vary according to the vessel type and size. The wall of large blood vessels has three main layers. The internal intima is composed of the inner endothelium and a subendothelial connective tissue. The internal elastic lamina (IEL) delimits the intima from the media. The media is formed by layers of circumferential smooth muscle cells and connective tissue with fibers. The external elastic lamina (EEL) is located between the media and the adventitia. The adventitia mainly consists of connective tissue with some SMCs, nerves, vasa vasorum, and lymphatic vessels.

The media is the main site of histological specializations of artery walls. Vessels proximal to the heart are elastic arteries, involved in the windkessel effect. The thick media contains thin concentric fenestrated lamellae of elastin. EEL is not very well defined and the adventitia is thinner than in distal muscular arteries. Muscular arteries have thinner intima and a media which is characterized by numerous concentric layers of SMCs. EEL can be clearly observed.

The vein walls are thinner than artery walls, and the caliber is larger. The intima is very thin. IEL and EEL are either absent or very thin. The media is thinner than the adventitia. Medium-sized veins are characterized by the presence of valves in order to prevent the transient blood returning

to upstream segments during muscular compression. The largest veins have very thick adventitia, with bundles of longitudinal SMCs and vasa vasorum. Valves are absent.

Arterioles are composed of an endothelium surrounded by one or a few concentric layers of SMCs, which regulate blood flow. Capillaries are small exchange vessels composed of endothelium surrounded by basement membrane with three structural types: continuous capillaries have tight intercellular clefts; fenestrated capillaries are characterized by perforations in endothelium; and discontinuous capillaries are defined by large intercellular and basement membrane gaps. Venules are composed of endothelium surrounded by basement membrane for the postcapillary venules and smooth muscle for the larger venules.

2.5.4.1 Vascular Smooth Muscle Cell

The vascular smooth muscle cell, which contains α-smooth muscle actin, carries out slow and sustained contractions. Actin and myosin in SMCs are not arranged into distinct bands. SMC activity is regulated by $[Ca^{++}]_i$ due to Ca^{++} entry via VDCCs, to Ca^{++} release from endoplasmic reticulum, and to receptor-dependent Ca^{++} channels. Vasodilator and vasoconstrictor influences are exerted upon a basal vascular tone. A vasomotor tone is indeed spontaneously developed in most arterioles [DUa]. In isolated arterioles and arteries, the basal tone is developed for vessel physiological pressure [DAa].

Myosin light chain (MLC) phosphorylation, which leads to the contraction, is tightly controlled by the relative activities of the counterregulatory enzymes myosin light chain kinase (MLCK) and myosin phosphatase. MLCK is activated by calcium and calmodulin. Caldesmon is a calmodulin-binding protein implicated in the regulation of actomyosin interactions. Calponin, a Ca^{++} and calmodulin-binding troponin T-like protein, binds to tropomyosin and to calmodulin. MLC phosphorylation leads to cross-bridge formation between the myosin heads and the actin filaments, and hence, to smooth muscle contraction. Dephosphorylation of myosin light chains by PKC leads to relaxation. The cGMP-dependent protein kinase 1α mediates SMC relaxation [SUa]. The RhoA pathway inhibits the myosin phosphatase.

2.5.4.2 Pericytes

The pericytes, which surround the capillaries, can also encircle precapillary arterioles and postcapillary venules. A basal lamina separates the endothelial cells and the pericytes. However, tight and gap junctions can develop between the endothelial cells and the pericytes. A basement membrane can also be found along the outer surface of the pericytes. The

pericytes regulate the capillary bore and, then, the tissue perfusion, as well as the transport from the blood via pericytic processes at interendothelial clefts. The pericytes secrete vasoactive autoregulating substances and release structural constituents of the basement membrane and interstitial matrix. Pericyte coverage is required during angiogenesis.

2.5.4.3 Endothelial Cells

The endothelium is involved

1. In blood-wall exchange control
2. In vasomotor tone modulation
3. In coagulation regulation
4. In vessel wall growth and remodeling
5. In inflammation and immune pathways, driving the leukocyte adhesion

The wetted cell membrane is covered by the glycocalyx, made of proteoglycans, glycosaminoglycans, glycoproteins, and glycolipids. The glycocalyx is the first barrier to molecular transport from the flowing blood.

2.5.4.4 Mechanotransduction

The shear stress and the pressure exerted on the wall by the blood generate a basal tone of SMCs in the absence of neurogenic and hormonal influences. The hemodynamic stresses act on the smooth muscle cells via stress transmission or via compound release by the endothelial cells. The endothelial membrane is the first wall component to bear stresses from the circulating blood. Stresses can act on mechanosensitive ion channels, on cell-membrane receptors, on adhesion molecules, on proteins associated with cytoskeleton proteins, on elements of cell junctions, and so on. These changes lead to biochemical responses.

In vitro effects of flow over a cultured EC layer and cyclic stretch of the culture support have been investigated to study the responses of endothelial cells in well-defined mechanical conditions. Support and perfusion media used in flow chambers can introduce substances that can interfere with the cell response to the investigated stimulus. Consequently, experimental testing and result interpretation must be carefully handled.

Stresses applied on EC wetted or on abluminal surface affect

1. The cell shape and orientation [DEe], as well as the cell ultrastructure [NOc]

2. The cell rheology [THa, SAc], the endothelial cell becoming stiffer

3. Cell proliferation

4. Cell metabolism and transport

5. Cell adhesion to its support and the matrix content

Endothelial cells respond, in particular, to space and time changes in wall shear stress (WSS). Studying the responses of the endothelial cells to step flows, impulse flows, ramp flows, inverse ramp flows, and pulsatile flows, it has been shown that the time derivative of WSS, and not the shear stress itself, is directly responsible for the EC reactions [BAa].

Nitric oxide. NO is a vasodilator and inhibits vasoconstrictor influences. NO also inhibits platelet and leukocyte adhesion to the endothelium. NO has an antiproliferative effect on SMCs. It is produced from L-arginine by nitric oxide synthase (NOS, Figure 2.5). There are two isoforms of NOS: constitutive (cNOS) and inducible (iNOS). NO is continuously produced. Its release is enhanced by multiple stimuli. NO acts via cGMP, after binding to guanylyl cyclase. cGMP decreases Ca^{++}/Cam stimulation of myosin light chain kinase. NO can be released from the endothelium by α 2-adrenoceptor activation, serotonin, aggregating platelets, leukotrienes, adenosine diphosphate, and bradykinin [VAc]. Hypoxemia also yields vasodilatation [POa]. The time gradients of the wall shear stress induce transient high-concentration burst of NO release via G proteins [BAa].

Endogenous NO contributes to CMC "hibernation" by reducing oxygen consumption and preserving calcium sensitivity and contractile function without an energy cost during ischemia [HEe]. The endothelium and the myocardium then are able to adapt to ischemia. The hypoxemia also induces the production of prostaglandins PGE2 and leukotriens LktC4 by CMCs.

Endothelin. The endothelin (ET) is a potent vasoconstrictor. It also regulates the extracellular matrix synthesis by stimulated vascular smooth muscle cells (Figure 2.6). In human myocardium in vitro, endothelin exerts a positive inotropic effect via sensitization of cardiac myofilaments to calcium and activation of the sodium exchanger [PIa]. However, the generated coronary vasoconstriction balances the positive inotropic and chronotropic effects. Endothelin is also a growth factor for cardiomyocytes [ITa]. The ET-1 release is shear-dependent [MOa].

Other vasoactive substances. Prostacyclin (PGI2) is another endothelium-derived vasodilator. Endothelium-derived hyperpolarizing factor (EDHF) can also be a prominent vasodilator hampered by NO. The endothelial

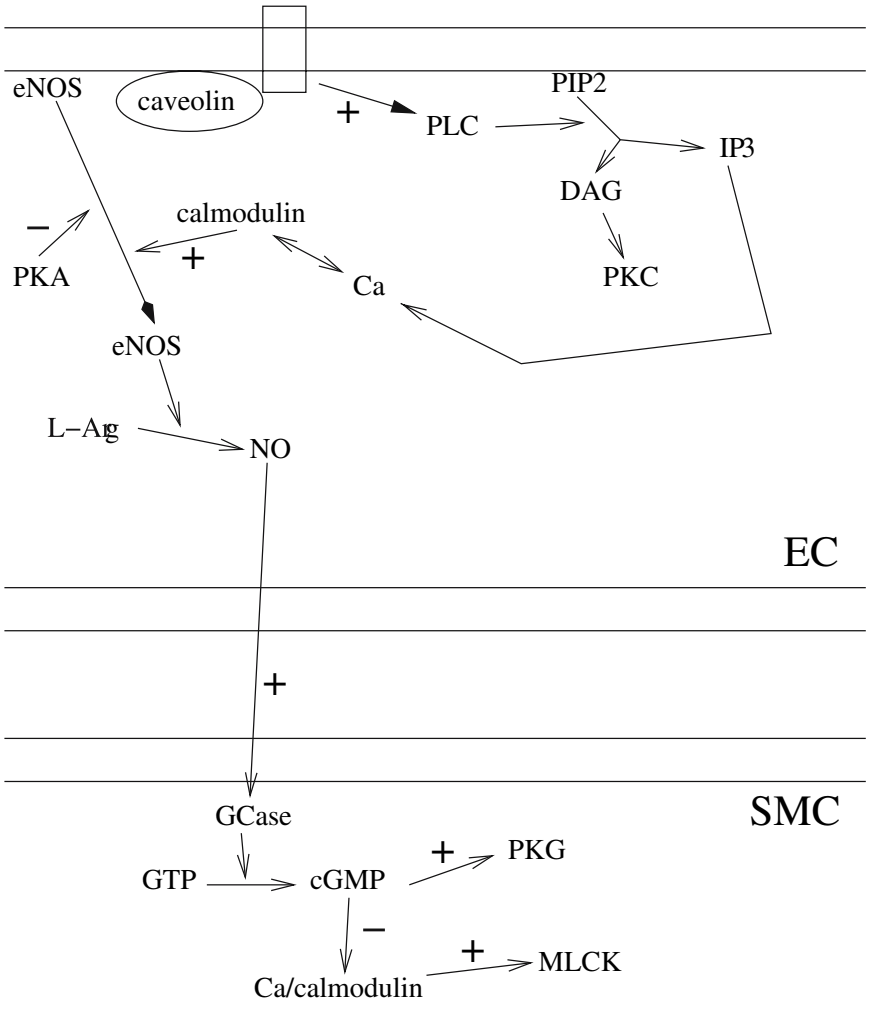

Figure 2.5. Nitric oxide (NO) produced in the endothelial cells by nitric oxide synthase (eNOS). eNOS is bound to caveolin in the cell membrane (inactive state). Activation of phospholipase C (PLC) by the ligand-bound receptor produces inositol triphosphate (IP3) and diacylglycerol (DAG) from phosphatidylinositol biphosphate (PIP2). IP3 increase in intracellular calcium content, which activates calmodulin. The latter dissociates eNOS from caveolin (cytosolic translocation). Protein kinase A (PKA) inactivates eNOS, which then relocates to the membrane caveolin (source: www.sigmaaldrich.com). NO stimulates guanylyl cyclase (GCase). cGMP decreases the stimulation by the Ca/calmodulin complex of myosin light chain kinase (MLCK) and activates protein kinase G (PKG).

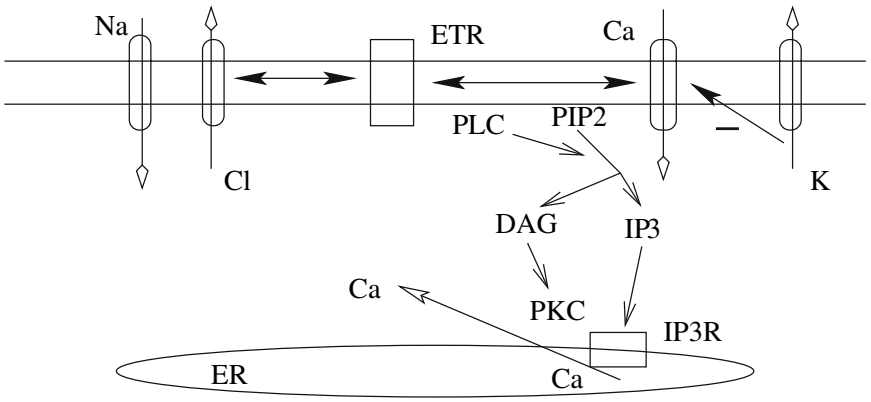

Figure 2.6. Binding of endothelin 1 to its receptor (ETR) induces activation of phospholipase C (PLC), which degrades phosphatidylinositol bisphosphate (PIP2) into diacylglycerol (DAG) and inositol trisphosphate (IP3). IP3 links to its receptor (IP3R) on the endoplasmic reticulum (ER) in order to release calcium (Ca) from ER. DAG activates protein kinase C (PKC). ETR is associated with a calcium channel of the cell membrane, which opens in response to ETR binding, hence further increasing the cytosolic calcium content. ET also opens chloride (Cl, Cl^- efflux), sodium (Na, Na^+ influx) and potassium (K, K^+ efflux) channels. K^+ efflux inhibits the Ca channel (Source: www.sigmaaldrich.com).

cells also produce endothelium-derived contracting factors, which include superoxide anions [KAa], endoperoxides, and thromboxane A2.

The uridine adenosine tetraphosphate (Up4A) vasoconstricts the blood vessel.

Myogenic response. The myogenic response, independent of the vascular endothelium, couples SMC contraction or relaxation to SMC deformation [JOa]. Stresses can act

1. On exchangers and transporters
2. On membrane ion channels
3. On membrane bound enzymes to modulate activity of contractile proteins

Ca^{++} influx leads to phospholipase C activation and release of inositol triphosphate and diacylglycerol [SHa]. Protein kinase C is involved in the myogenic response in the microcirculation [MEb]. The phosphatidylinositol metabolism stimulated by mechanical factors enhances $[Ca_i^{++}]$ and causes a translocation of PKC from cytosol to membrane [NOc].

2.5.5 Vessel Wall Rheology

The vessel walls exhibit longitudinal and circumferential prestresses. In vitro rheology measurements on excised or isolated vessels need suitable vessel conservation and preconditioning. Various experimental methods have been developed; they are summarized in a literature review [HAa]. Uniaxial loading is widely used because carefully controlled 2-D/3-D experiments are difficult to carry out on biological tissues. Rheological properties differ whether tests are performed on isolated segments of the vasculature or in vivo. In in vitro experiments, connections and interactions between regions of the anatomical system and between the wall and its neighborhood are removed, although they affect the wall rheology. Furthermore, excised tissues are more or less dried and not perfused. Conversely, in vivo measurements are carried out in a noisy environment due to blood circulation and respiration on targeted regions of limited surface areas, most often without preconditioning and without control of influence factors.

Imaging velocimetry (US, MRV) can be used as indirect methods. Two exploring stations are not sufficient because a single value of the wave speed does not take into account the nonlinear pressure-dependency of the wave speed. It has been proposed to use three stations, two giving the BCs, and one the pressure-dependency, assuming a 1-D flow. It is also possible to process the pressure signals from two stations in three identifiable wave points (foot, peak, notch) with different time delay between the two waves, the absence of reflexion being assumed [STb]. With aging, the wall becomes stiffer and the wave speed increases. Besides, MRI shows that the wall deformation is not uniform as well as the circumferential variation in wall strains during the cardiac cycle [DRa]. Moreover, the muscular tone affects the vessel compliance, especially in muscular arteries and arterioles.

Uniaxial loadings exhibit nonlinear force-deformation relationships. Stress–strain relationships have been mainly explained by the wall microstructure. The ability to bear a load is mostly done by elastin and collagen fibers. The nonlinearity is commonly understood as an initial response of elastin fibers and a progressive recruitment of collagen fibers. At low strain, collagen fibers are not fully stretched and elastin fibers play a dominant role. At high strain, the higher stiffness of the stretched collagen fibers affects the elastic properties [FUb]. When the elastin content is higher than the collagen one, the elastic modulus decreases and distensibility increases and vice versa.

Constitutive equations are based on the strain energy function (SEF), which links stresses to strains via a differentiation. Logarithmic and exponential formulation have been proposed in the literature, but they are not fully appropriate for numerical simulations. Polynomial expressions

are prefered. The vessel wall can be considered as made of three elements, elastine, collagen (the response of which depends on the fiber stretch level), and SMCs (the response of which depends on deformation-dependent tone level) [ZUb]. Usually, the collagen fibers, embedded in the ground matrix and undulated in the rest configuration, are supposed to be gradually recruited. The vessel wall has been modeled as an isotropic elastic material containing an anisotropic helical network of stiff collagen fibers with a given orientation with respect to the circumferential direction [HOb].

Constrained mixture models, which meld classical mixture and homogenization theories, consider the specific turnover rates and configurations of the main constituents to study stress-dependent wall growth and remodeling [HUa, GLa]. But, appropriate knowledge of constituent material properties is still lacking.

2.5.6 Growth, Repair, and Remodeling

The growth and the remodeling of the wall of the vasculature (heart, blood vessels) are controlled. The processes, modulated by biomechanical quantities, are coordinated by biochemical mechanisms requiring factors and signals.

2.5.6.1 Growth Factors

Tissue growth needs mechanical, electrical, structural, and chemical signals to grow into functional 3-D tissue. Interactions of cells with ECM provide structural cues for normal cellular activity. Cell responses to various environmental signals are mediated by growth factors (GF). GFs promote not only cell meiosis, maturation, and functioning, but also tissue growth and remodeling. Cell growth is controlled by a balance between growth-promoting and growth-inhibiting factors. GFs can have autocrine, paracrine, juxtacrine, or endocrine effect (Figure 2.7). The epidermal growth factor (EGF) has proliferative effects especially on fibroblasts. The platelet-derived growth factor (PDGF), fibroblast growth factor (FGF), and vascular endothelial growth factor (VEGF) are involved in angiogenesis (Figure 2.8). The transforming growth factor-β is a growth inhibitor for endothelial cells and fibroblasts. Cytokines are growth factors that modulate activities of immune cells. Interleukins (IL) are growth factors targeted to hematopoietic cells. Interferons (IFN) are cytokines produced by the cells of the immune systems in response to foreign agents. Sphingosine 1-phosphate (S1P), a lipid growth factor, mediates locomotion and maturation of endothelial cells. Endothelial cells have an intracellular reserve of functional S1P1 in caveolae. S1P acts on various pathways via

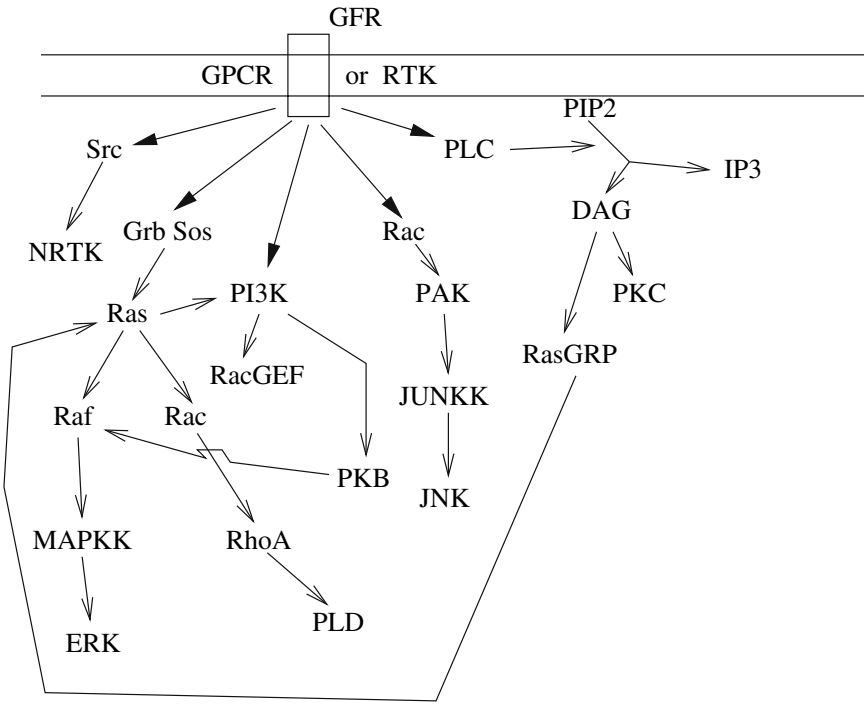

Figure 2.7. Growth factor-bound receptor activates adaptor protein Grb coupled to the guanine nucleotide releasing factor Sos (Grb–Sos complex), and, subsequently Ras, Raf, mitogen-activated protein kinase (MAPK), and extracellular regulated kinase (ERK) and Rac, RhoA, and PLD on the other hand. Ligand-bound receptors also activate (1) phosphatidylinositol 3-kinase (PI3K), protein kinase B (PKB), (2) Src, (3) Rac and JNK, and (4) phospholipase C (PLC) (Source: www.sigmaaldrich.com).

G-protein-coupled receptors (GPCR, Figure 2.9). S1P tightens adherens junctions between endothelial cells, characterized by VE cadherins.

2.5.6.2 Chemotaxis

Chemotaxis requires several main processes:

1. Cell alignment along the chemoattractant gradient
2. Cell polarization
3. Protrusion at the leading edge (cell front) and retraction at the trailing edge (cell back) of cytoskeletal elements, which all implicate small GTPases [MEa]

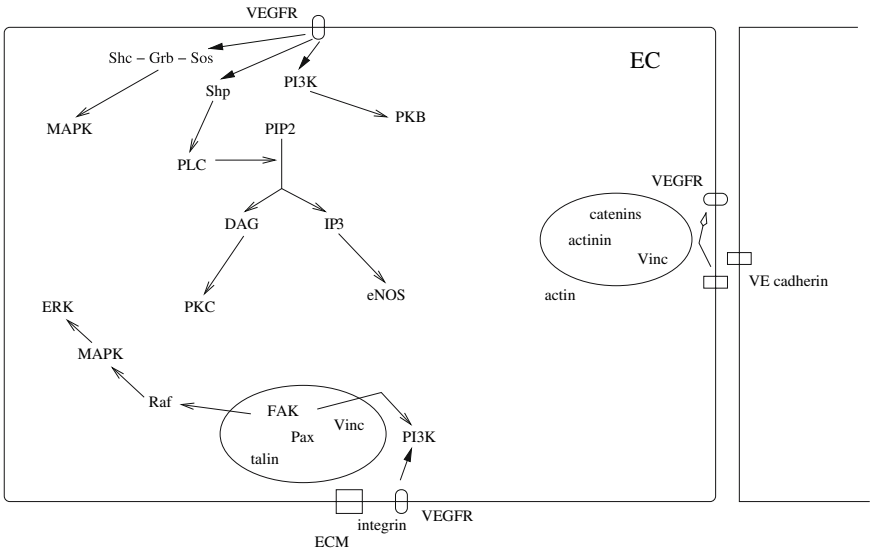

Figure 2.8. The vascular endothelial growth factor (VEGF) stimulates angiogenesis, particularly proliferation of endothelial cells (EC). VEGF binds to its receptors (VEGFR-1, VEGFR-2, VEGFR-3). It then activates a cell type-dependent signaling cascade via Shc and Grb, tyrosine phosphatases Shp and PLC-γ, phosphatidylinositol 3-kinase (PI3K), and so on. Vascular endothelial (VE)-cadherins are involved in the adherens junctions between neighboring ECs. VE-cadherins interact with catenins, and, subsequently, with α-actinin and vinculin (Vinc), and with the actin cytoskeleton. VE-cadherin acts with VEGFR-2 to control the PI3K/PKB pathway. ECs are linked to the extracellular matrix (ECM) via integrins, such as $\alpha_v\beta_3$ and focal adhesion molecules, such as focal adhesion kinase (FAK), talin, paxillin (Pax), and Vinc (Source: www.sigmaaldrich.com).

The chemotactic flux depends

1. On a chemotactic response function of the available cell number and of the chemoattractant concentration
2. On chemoattractant concentration gradient [MUa]

The time gradient of the chemoattractant concentration depends on the production and destruction rates as well as its diffusion flux. The Keller–Segel model is widely used for the chemical control of cell movement [KEa]. A new formulation of the system of partial differential equations has been obtained by the introduction of a new variable and is approximated via a mixed finite element technique [MAb]. Chemotaxis is used in vasculogenesis and angiogenesis [AMa].

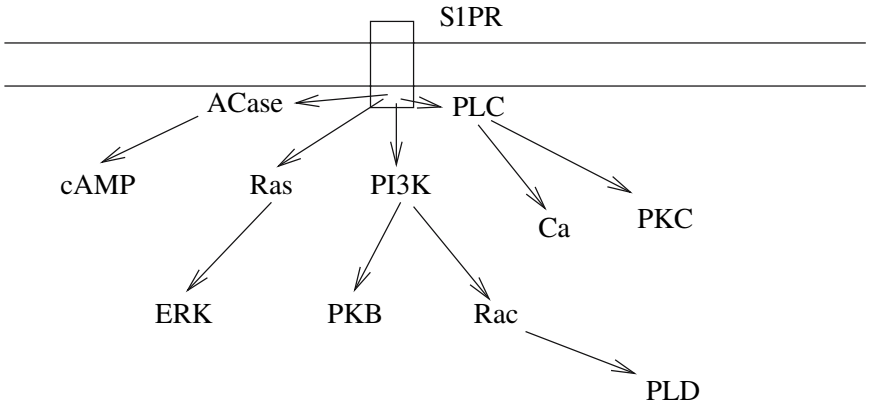

Figure 2.9. Sphingosine 1-phosphate (S1P) is produced intracellularly and is then secreted. It acts on adenylyl cyclase (ACase), Ras, phosphatidylinositol 3-kinase (PI3K), and phospholipase C (PLC).

2.5.6.3 Growth and Repair

Vasculogenesis defines formation of capillary plexus from endothelial stem cells (embryological process). A primitive vascular network is formed during embryogenesis through the assembly of angioblasts. Angiogenesis is characterized by maturation of or generation from a primary vascular network. Arteriogenesis deals with formation of mature arterioles and arteries with SMCs, for example, for collateral development in order to bypass an obstructed artery. Blood and the vessel wall are also involved in defense and repair processes. Both chemotaxis (directed response of cells according to a chemoattractant concentration gradient) and haptotaxis (adhesion gradient associated with the concentration of the constituent of the support medium, i.e. gradient of extracellular matrix density) are involved during the tissue development.

Vasculogenesis. During vasculogenesis, angioblasts differentiate and determine "blood pockets" which lengthen to form irregular capillaries. These pipes connect to each other in a nonhierarchical inhomogeneous network of primitive vessels. Once associated with the heart pump, this network, which conveys moving blood, remodels with branching. Vessels through which blood flows with high and/or quick flow rates widen and narrow. The network progressively matures with arteries, capillaries, and veins [LEb].

Optimal design of vessel branching is based on cost functions that are the sum of the rate at which work is done on blood and the rate at which energy is used, supposedly proportional to the vessel volume for each vessel segment [MUa]. Other cost functions have been proposed, based on the

minimal total surface area of blood vessels, the minimal total volume, or the minimal total wall shear force on the vessel wall or the minimal power of the blood flow.

Angiogenesis. Angiogenesis is a process leading to the generation of blood vessels through sprouting from existing blood vessels, because it involves migration and proliferation of endothelial cells from preexisting vessels. Localized production of growth factors promotes tissue expansion and determination of the position of branching nodes, with possible adaptation. The formation of new blood vessels or the remodeling of existing blood vessels requires the controlled growth of various cell types by different factors. Development of vascular trees also includes wall stress adaptation mechanisms. Limitation in angiogenesis is provided by angiostatin and endostatin. Antiangiogenic compounds are useful in cancers, such as inhibitors

1. Of ECM remodeling
2. Of adhesion molecules
3. Of activated endothelial cells
4. Of angiogenic mediators or receptors

Angioinhibins and other factors negatively influence angiogenesis, either by inhibiting endothelial cell proliferation or by preventing cell migration.

Arteriogenesis. Once the lumen of a main artery narrows too much, the lumen of a small artery increases to form a collateral in order to maintain the blood flow. Arteriogenesis is initiated by the monocyte chemoattractant protein-1 (MCP1) [VAb]. Various substances are also required at different stages of arteriogenesis; among these, TGFβ, PDGF, FGF2, GM-CSF, and TNF-α. Attracted monocytes produce fibronectin and proteoglycans as well as proteases in order to remodel the extracellular matrix. These inflammatory cells then produce growth factors to stimulate EC and SMC proliferation.

Stem cells. Stem-cell revascularization for tissue oxygenation and myocardium regeneration for pump functioning are proposed therapies. However, cell therapy can be ineffective or even hazardous in certain clinical settings and in specific subgroups of patients [HIa, HEb]. In the heart, resident stem cells can lead to endothelial cells, smooth muscle cells, and cardiomyocytes [BEa].

Tissue engineering. Bioreactors are devices used for the growth of tissues in an artificial environment that mimics the physiological conditions. In vivo biomechanical and chemicophysical conditions are created for in vitro cell

conditioning and for construction of blood vessel, heart valves, and so on, with similar features to the native tissue ones. Histological niches, which define the cell status, its living site, its functioning, and its interactions with the environment, must then be replicated in bioreactors.

In planar cultures on matrices rich in collagen IV and laminin, the endothelial cells form clusters and pull on the matrix, generating tension lines that can extend between the cell aggregates. The matrix eventually condenses along the tension lines, along which the cells elongate and migrate, building cellular rods. The rate of change in cell density is equal to the balance between the convection and the strain-dependent motion. The inertia being negligible, the forces implicated in the vasculogenesis model include the traction exerted by the cells on the ECM, the cell anchoring forces, and the recoil forces of the matrix [MUb]. In order to study the role of the mechanical and chemical forces in blood vessel formation, a mathematical model has been developed using a finite difference scheme to simulate the formation of vascular networks in a plane [MAa]. The numerical model assumes

1. Traction forces exerted by the cells onto the extracellular matrix
2. A linear viscoelastic matrix
3. Chemotaxis

Spontaneous formation of networks can be explained via a purely mechanical interaction between the cells and the extracellular matrix.

Myocardium remodeling. Acute myocardial infarction leads to necrosis of cardiomyocytes and other cells. The heart contains rare cardioblasts susceptible to division, for self-regeneration and maturation [LAa]. CMC proliferation, from CMCs, resident stem cells, endothelial cells, fibroblasts, or migrated hematopoietic stem cells, in an area adjacent to the infarcted zone can be a regeneration source. Adequate input in growth factors is necessary to stimulate myocardial regeneration with needed angiogenesis and ECM formation in order to avoid maladaptive remodeling of the myocardium. Cardiac hypertrophy is induced by sustained pressure overload. Multiple hypertrophy signaling pathways are triggered by the pressure: calcineurin, phosphoinositide-3 kinase/protein kinase B, and ERK1/2.

Wall remodeling. Blood vessels are subjected to mechanical forces that regulate vascular development, adaptation, and genesis of vascular diseases. A chronic increase in arterial blood flow leads to vessel enlargement and reduction in WSS to physiological values. Wall remodeling is characterized by SMC proliferation and migration. Wall remodeling implies changes in rheological properties, and, consequently, the material constants of the constitutive law must be updated. Moreover, the constitutive equation must

include not only the stress history but also material history due to wall restructuralization.

Flow-induced changes involved in long-term vascular tissue growth and remodeling have been studied using the continuum approach and motion decomposition [HUa, HUb]. The proposed homogenized, constrained mixture theory is used to develop a 3-D constitutive law that takes into account the three primary load-bearing constituents (SMC, collagen, and elastin) with time-varying mass fractions due to the turnover of cells and extracellular matrix fibers during the wall remodeling under a varying stress field. The turnover of constituent i is described by its total mass evolution, introducing two evolution functions for production and for degradation rates. Besides, axial extension quickly increases the length of a carotid artery and the rate of turnover of cells and matrix, the turnover rates correlating with the stress magnitude. Numerical simulations show that moderate (15%) increases in axial extension generate much greater axial stress than circumferential stress augmentation induced by marked (50%) rise in blood pressure [GLb]. A 2-D constrained mixture model, based on different constitutive relations, shows that the turnover of cells and matrix in altered configurations is effective in restoring nearly normal wall mechanics.

2.6 Cardiovascular Diseases

Cardiovascular diseases can develop because of a favorable genetic ground and of exposure to risk factors. They are primarily located either in the blood vessels, mainly the arteries, or in the heart. Due to the lack of space, this review is only focused on two major arterial pathologies, the aneurisms and atherosclerosis. Both wall diseases are targeted by physical and mathematical modeling and by mini-invasive treatments, coiling and stenting.

2.6.1 Atheroma

Atherosclerosis is defined by a deposition of fatty materials and then fibrous elements in the intima, beneath the endothelium. The artery wall thickens and the lesion secondarily protudes into the lumen. Atheroma may be scattered throughout the large and medium thick-walled systemic arteries, especially in branching regions. The inflammation is composed of four main stages characterized by

1. Foam cells
2. Fatty streaks

3. Intermediate lesions

4. Uncomplicated, then complicated, plaques

When atherosclerosis begins, LDL, which have crossed the endothelium, are oxidized in the intimal connective layer. These modified LDL induce an immune response. Attracted monocytes and T-lymphocytes migrate from the blood stream into the artery wall. Migrated monocytes multiply and are transformed into macrophages with scavenger receptors at the cytoplasmic membrane. Oxidized LDL (oxLDL) are bound to the scavenger receptors and then ingested by the macrophages. Ingestion of oxLDL is unsaturatable and leads to foam cell formation. OxLDL and proinflammatory cytokines induce expression of adhesion molecules, and cell chemotaxis. Secreted chemokines, such as macrophage chemoattractant protein (MCP), and growth factors stimulate the migration of smooth muscle cells from the media to the intima. SMCs can dedifferentiate, losing their contractile properties. Dysfunctional SMCs contribute to lipid accumulation and calcification in the atherosclerotic plaque. Agglomeration of foam cells, of T-lymphocytes, of SMCs, with extracellular matrix synthesis forms fatty streaks. The streaks gradually become larger, covered by a fibrous cap. The fibrous cap increases and a necrotic core can occur. Episodic fibrous cap ruptures initiate thrombus formations.

Mediators of immunity are involved at various stages of atherosclerosis. Ceramide is implicated in atherogenesis. Following uptake by the endothelial cells (EC), a part of the LDL-derived ceramide is converted into sphingosine, whereas another part accumulates inside the cells, with an increased rate of apoptosis [BOf]. Oxidative stress, a consequence of hypoxemia, is implicated in atherosclerosis. Statins are regulators of NO synthesis by ECs. They inhibit leukocyte transmigration [SAb]. Apolipoprotein E regulates the cholesterol metabolism. Its level decay increases atherosclerosis risk.

Various works were performed to discover which blood dynamic factors participate in atherogenesis. Strong correlation has been found between low wall shear stress (WSS) region and atherosclerotic plaque localization [CAf]. The atherosclerosis mainly occurs not only where WSS is low, but also where WSS strongly changes both in time and in space. Intimal thickening may correspond to a remodeling response. Secondarily, a lesion can develop, caused by disturbed transmural fluxes of cells and lipoproteins. The stresses applied by the blood flow on the vessel wall are involved in the pathogenesis as well as in complications, such as damage of the fibrous cap and cracking of the plaque. Investigations have been mostly performed in idealized geometry, assuming rigid walls due to atheroma-induced hardening and passive homogeneous plaques. In any case, accumulation of lipidic molecules is not only secondary to increased influx with changes

in endothelial permeability, but is also the consequence of decreased wall efflux, especially by the microcirculation of the outer half of the vessel wall.

The stenosis induces ischemia and tissue infarction, most often by a distal flow blockage by emboli. Flow perturbations induced by a severe lumen narrowing can be detected by ultrasound techniques. The systolic jet through the stenosis is associated with recirculation zones. Flow separations can also be produced during the diastole. The blood stagnation or, at least, low-speed transport can more easily trigger clotting on the more or less damaged endothelium of the constricted segment.

2.6.2 Aneurism

The aneurism is the product of a multifactorial process that leads a gradual dilation of an arterial segment over years. The aneurism wall stretches and becomes thinner and weaker than normal artery walls. Consequently, an untreated aneurism can rupture. Two main kinds of aneurisms exist, fusiform wall dilation and saccular bulging of the artery wall. Fusiform aneurisms are often complications of atheroma. Saccular aneurisms can occur after an infection or a traumatizing of the wall, whereas congenital aneurisms are located at the branching sites of the brain arterial network.

A mechanically induced degeneration of the wall internal elastic lamina has thus been proposed as the initiating cause of congenital aneurisms with genetic predisposition. Imbalance between matrix metalloproteinases (MMP) and their inhibitors, the tissue inhibitors of metalloproteinases (TIMP), are involved in formation of abdominal aortic aneurisms (AAA). AAAs are characterized by chronic inflammation, destructive remodeling of the extracellular matrix, and increased activity of MMPs [IRa]. In AAAs, the volume fraction of elastin and of SMCs decreases and the combined content of collagen and ground substance increases [HEa]. The percentage of chondroitin sulphate increases and that of heparan sulphate decreases [SOa].

In clinical practice, the rupture risk must be estimated. Stress distribution in the aneurism is investigated to find regions subjected to high stresses and to plan the treatment accordingly. The geometry of the aneurism can be reconstructed from patient 3-D images. Experiments and numerical simulations have been mostly carried out in AAAs and intracranial saccular aneurisms (ISA), focused on the stress field either in the lesion wall [RAb, DIa] or in the blood cavity [STa, BOb]. A saccular aneurism illustrates the help of numerical simulations for the choice of the treatment (Figure 2.10). The high-pressure zone in the neck gives an argument in favor of surgical clipping because the aneurism is superficial with easy surgical access. It is not possible, indeed, to protect the neck efficiently with coiling because coils in this location will always induce emboli. However, if the endovascular

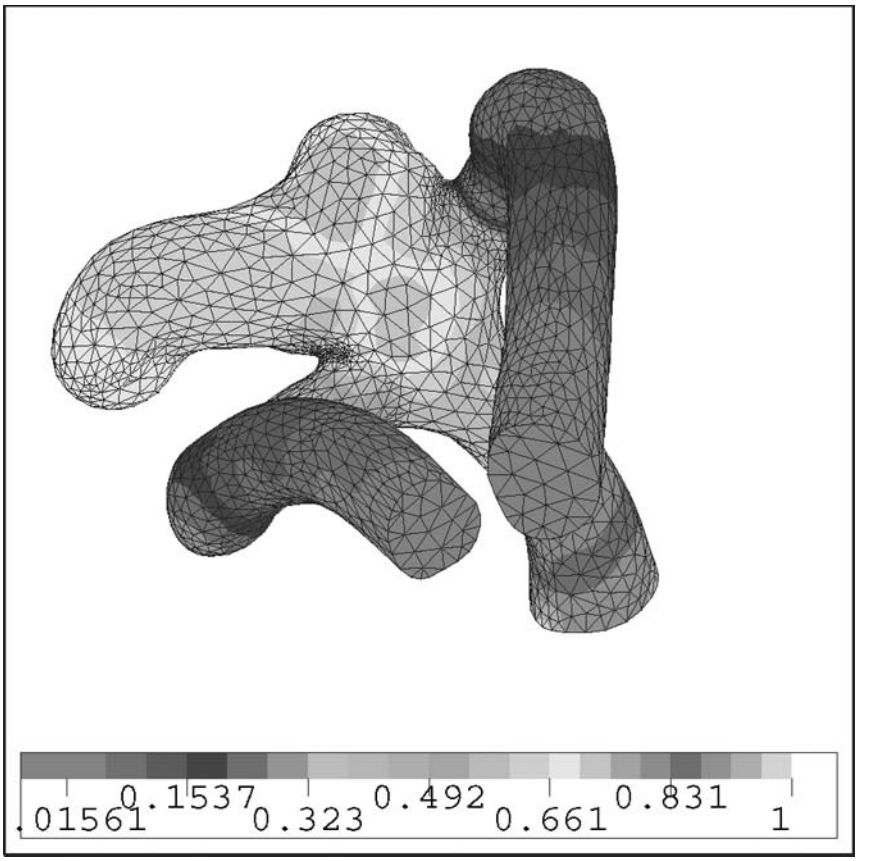

Figure 2.10. Pressure field in a terminal branching aneurism at peak flow.

treatment is chosen with respect to heavily invasive surgery, frequent angiography control must be done because of the high risk of recanalization. Model improvements are needed in order to take into account the aneurism wall responses to the stress field applied by the blood, at the tissue level as well as at the cell scale, both being associated with synthesis or degradation of multiple compounds.

2.7 Conclusion

Three-dimensional numerical modeling that completely describes the myocardium activity must couple models at various length scales in order to

take into account the biochemical machinery that triggers and is responsible for heart contractions. Such a coupling indeed involves

1. Electrochemical wave propagation
2. Myocardium contraction–relaxation
3. Blood systolic ejection, which is generated by the contraction of the whole left ventricle tuned by the action potential.

Future investigations are then aimed at developing patient-specific tools, which combine not only medical images but also physiological signals to the heart model. The complete heart model takes into account the metabolic (perfusion), the electrochemical, and the mechanical activities. Such a computer tool can be used to solve inverse problems in order to estimate parameters and state variables from observations of the cardiac function (data assimilation). The fluid dynamics within the coronary network, which irrigates the myocardium, can be based on a hierarchical approach, taking into account both the large coronary arteries and the intramural vessels. The three-dimensional blood flow model in distensible right and left coronary arteries (proximal part of the heart perfusion network, located on the heart surface) can be coupled with the one-dimensional flow model for wave propagation, which can correspond to the first six generations of branches [SMa], and a poroelastic model of the small arteries and the microcirculation which cross the heart wall, using homogenization [CIa, HUe], the wall permeability depending on the wall deformation. This hierarchical flow enumerate is coupled with oxygen transport.

Mechanotransduction is another example of intricate biomechanical reactions interlinked to biomechanical phenomena. The continuum level remains used at the cell scale to estimate the stress distribution in the wall layers of the vasculature and the interactions among the large cell components, the nucleus, the cytosol, and the membrane, the small cell organelles being neglected. Such interactions can affect the local flow and, consequently, mass transport and mechanotransduction. The mechanotransduction is investigated to clarify the manifold stress-induced processes from sensing to processing, and to better define the niches of the vascular cells. The better the niche, the more efficient is cell and tissue engineering for tissue replacement. Genes involved in mechanotransduction, coding for ion channels, or responsive substances are targets for additional studies.

Nowadays, biomechanical models are beginning to incorporate involved microscale events. Biomechanics also contributes to the development of new diagnosis methods, of new measurement techniques, from signal acquisition to processing, of new surgical or medical implantable devices, and of new therapeutic strategies.

2.8 References

[AAa] Aaron, B.B. and Gosline, J.M., Elastin as a random-network elastomer: a mechanical and optical analysis of single elastin fibers, *Biopolymers*, **20** (1981), 1247–1260.

[ALa] Aliev, R.R. and Panfilov, A.V., A simple two-variable model of cardiac excitation, *Chaos Solitons Fractals*, **7** (1996), 293–301.

[AMa] Ambrosi, D., Bussolino, F., Preziosi, L., A review of vasculogenesis models *Journal of Theoretical Medicine*, **6** (2005), 1–19.

[ANa] Anand, M. and Rajagopal, K.R., A mathematical model to describe the change in the constitutive character of blood due to platelet activation, *C.R. Acad. Sci. Paris*, Mécanique, **330** (2002), 557–562.

[AUa] Aumailley, M. and Gayraud, B., Structure and biological activity of the extracellular matrix, *J. Mol. Med.*, **76** (1998), 253–65.

[AZa] Azhari, H., Weiss, J.L., Rogers, W.J., Siu, C.O., Zerhouni, E.A., and Shapiro, E.P., Noninvasive quantification of principal strains in normal canine hearts using tagged MRI images in 3-D, *Am. J. Physiol.*, **264** (1993), H205–216.

[BAa] Bao, X., Lu, C., and Frangos, J.A., Mechanism of temporal gradients in shear-induced ERK1/2 activation and proliferation in endothelial cells, *Am. J. Physiol., Heart Circ. Physiol.*, **281** (2001), H22–29.

[BEa] Beltrami, A.P., Barlucchi, L., Torella, D., Baker, M., Limana, F., Chimenti, S., Kasahara, H., Rota, M., Musso, E., Urbanek, K., Leri, A., Kajstura, J., Nadal-Ginard, B., and Anversa, P., Adult cardiac stem cells are multipotent and support myocardial regeneration, *Cell*, **114** (2003), 763–776.

[BEb] Bestel, J., Clément, F., and Sorine, M., A biomechanical model of muscle contraction, In **Medical Image Computing and Computer-Assisted Intervention** (MICCAI'01), Lectures Notes in Computer Science, Niessen, W.J., and Viergever, M.A. eds, Springer-Verlag, New York (2001), 2208, pp. 1159–1161.

[BIa] Binning, G., Quate, C.F., and Gerber, C., Atomic force microscope, *Phys. Rev. Lett.*, **56** (1986), 930–933.

[BOa] Bogaert, J. and Rademakers, F.E., Regional nonuniformity of normal adult human left ventricle, *Am. J. Physiol., Heart Circ. Physiol.*, **280** (2001), H610–620.

[BOb] Boissonnat, J.D., Chaine, R., Frey, P., Malandain, G., Salmon, S., Saltel, E., and Thiriet, M., From arteriographies to computational

flow in saccular aneurisms: The INRIA experience, *Med. Image Anal.*, **9** (2005), 133–143.

[BOc] Bos, J.L., de Rooij, J., and Reedquist, K.A., Rap1 signalling: Adhering to new models. *Nat. Rev. Mol. Cell. Biol.*, **2** (2001), 369–77.

[BOd] Bourdarias, C., Gerbi, S., and Ohayon, J., A three dimensional finite element method for biological active soft tissue, *Math. Model. Numer. Anal.*, **37** (2003), 725–739.

[BOe] Bourgault, Y., Ethier, M., and LeBlanc, V.G., Simulation of electrophysiological waves with an unstructured finite element method, *Math. Model. Numer. Anal.*, **37** (2003), 649–661.

[BOf] Boyanovsky, B., Karakashian, A., King, K., Giltyay, N.V., and Nikolova-Karakashian, M., Ceramide-enriched low-density lipoproteins induce apoptosis in human microvascular endothelial cells, *J. Biol. Chem.*, **278** (2003), 26992–26999.

[BRa] Brookes, P.S., Yoon, Y., Robotham, J.L., Anders, MW., and Sheu, SS. Calcium, ATP, and ROS: A mitochondrial love-hate triangle, *Am. J. Physiol., Cell Physiol.*, **287** (2004), C817–C833.

[CAa] Caille, N., Thoumine, O., Tardy, Y., and Meister, J.J., Contribution of the nucleus to the mechanical properties of endothelial cells. *J Biomech.*, **35** (2002), 177–187.

[CAb] Caillerie, D., Mourad, A., and Raoult, A., Cell-to-muscle homogenization. Application to a constitutive law for the myocardium, *Math. Model. Numer. Anal.*, **37** (2003), 681–698.

[CAc] Cairns, C.B., Walther, J., Harken, A.H., and Banerjee, A., Mitochondrial oxidative phosphorylation thermodynamic efficiencies reflect physiological organ roles, *Am. J. Physiol., Regul. Integr. Comp. Physiol.*, **274** (1998), R1376–R1383.

[CAd] Canfield, T.R. and Dobrin, P.B., Static elastic properties of blood vessels, In: **Handbook of Bioengineering**, Skalak, R. and Chien, S. Eds., McGraw-Hill, New-York (1987), pp. 16.1–16.28.

[CAe] Carnegie, G.K. and Scott, J.D., A-kinase anchoring proteins and neuronal signaling mechanisms, *Genes Dev.*, **17** (2003), 1557–1568.

[CAf] Caro, C.G., Fitzgerald, J.M., and Schroter, R.C., Atherosclerosis and arterial wall shear: observations, correlation and proposal of a shear dependent mass transfer mechanism for atherogenesis, *Proc. Royal Soc. London B*, **177** (1971), 109–159.

[CHa] Chang, L., and Karin, M., Mammalian MAP kinase signalling cascades, *Nature*, **410** (2001), 37–40.

[CHb] Chapelle, D., Clément, F., Génot, F., Le Tallec, P., Sorine, M., and Urquiza, J., A physiologically-based model for the active cardiac

muscle, Lectures Notes in Computer Science, Katila, T., Magnin, I.E., Clarysse, P., Montagnat, J., and Nenonen, J. Eds, Springer-Verlag New York (2001), pp. 2230,

[CHc] Chien, S., Shear dependence of effective cell volume as a determinant of blood viscosity, *Science*, **168** (1970), 977–978.

[CIa] Cimrman, R. and Rohan, E., Modelling heart tissue using a composite muscle model with blood perfusion, in: **Computational Fluid and Solid Mechanics**, Bathe, K.J., Ed., Elsevier (2003).

[CIb] Civelekoglu, G. and Edelstein-Keshet, L., Modelling the dynamics of F-actin in the cell, *Bull. Math. Biol.*, **56** (1994), 587–616.

[CLa] Clark, E.A. and Brugge, J.S., Integrins and signal transduction pathways: The road taken, *Science*, **268** (1995), 233–239.

[CLb] Clark, R.A., Wikner, N.E., Doherty, D.E., and Norris, D.A., Cryptic chemotactic activity of fibronectin for human monocytes resides in the 120-kDa fibroblastic cell-binding fragment, *J. Biol. Chem.*, **263** (1988), 12115–12123.

[COa] Colli-Franzone, P., Guerri, L., and Tentoni, S., Mathematical modeling of the excitation process in myocardial tissue: Influence of fiber rotation on the wavefront propagation and potential field, *Math. Biosci.*, **101** (1990), 155–235.

[DAa] Davis, M.J., Kuo, L., Chilian, W.M., and Muller, J.M., Isolated, perfused microvessels, In **Clinically Applied Microcirculation Research**, Barker, J.H., Anderson, G.L. and Menger, M.D. eds, CRC, Boca Raton, 1995, pp. 435–456.

[DEa] de Bold AJ., Atrial natriuretic factor: A hormone produced by the heart. *Science*, **230** (1985), 767–770.

[DEb] de Brabander, M.J., Le cytosquelette et la vie cellulaire, *La Recherche*, **145** (1993), 810–820.

[DEc] Delhaas, T., Arts, T., Prinzen, F.W., and Reneman, R.S., Relation between regional electrical activation time and subepicardial fiber strain in the canine left ventricle, *Pflugers Arch.*, **423** (1993), 78–87.

[DEd] Dembo, M., The mechanics of motility in dissociated cytoplasm. *Biophys. J.*, **50** (1986), 1165–1183.

[DEe] Dewey, C.F., Bussolari, S.R., Gimbrone, M.A., and Davies, P.F., The dynamic response of vascular endothelial cells to fluid shear stress, *J. Biomech. Eng.*, **103** (1981), 177–185.

[DIa] Di Martino, E.S., Guadagni, G., Fumero, A., Ballerini, G., Spirito, R., Biglioli, P., and Redaelli, A., Fluid-structure interaction within realistic three-dimensional models of the aneurysmatic

aorta as a guidance to assess the risk of rupture of the aneurysm, *Med. Eng. Phys.*, **23** (2001), 647–655.

[DRa] Draney, M.T., Herfkens, R.J., Hughes, T.J., Pelc, N.J., Wedding, K.L., Zarins, C.K., and Taylor, C.A., Quantification of vessel wall cyclic strain using cine phase contrast magnetic resonance imaging, *Ann. Biomed. Eng.*, **30** (2002), 1033–1045.

[DUa] Duling, B.R., Gore, R.W., Dacey, R. G., and Damon, D.N., Methods for isolation, cannulation, and in vitro study of single microvessels, *Am. J. Physiol., Heart Circ. Physiol.*, **241** (1981), H108–H116.

[DUb] Durrer, D., van Dam, R.T., Freud, G.E., Janse, M.J., Meijler, F.L., and Arzbaecher, R.C., Total excitation of the isolated human heart, *Circulation*, **41** (1970), 899–912.

[EVa] Evans, E.A., New membrane concept applied to the analysis of fluid shear- and micropipette-deformed red blood cells, *Biophys. J.*, **13** (1973), 941–54.

[FAa] Fahraeus, R. and Lindqvist, T., The viscosity of the blood in narrow capillary tubes. *Am. J. Physiol.*, **96** (1931), 562–568.

[FAb] Faris, O.P., Evans, F.J., Ennis, D.B., Helm, P.A., Taylor, J.L., Chesnick, A.S., Guttman, M.A., Ozturk, C., and McVeigh, E.R., Novel technique for cardiac electromechanical mapping with magnetic resonance imaging tagging and an epicardial electrode sock, *Ann. Biomed. Eng.*, **31** (2003), 430–440.

[FIa] FitzHugh, R., Impulses and physiological states in theoretical models of nerve membrane, *Biophys. J.*, **1** (1961), 445–466.

[FOa] Fogel, M.A., Weinberg, P.M., Hubbard, A., and Haselgrove, J., Diastolic biomechanics in normal infants utilizing MRI tissue tagging, *Circulation*, **102** (2000), 218–224.

[FOb] Fogelson, A.L. and Guy, R.D., Platelet-wall interactions in continuum models of platelet thrombosis: Formulation and numerical solution, *Math. Med. Biol.*, **21** (2004), 293–334.

[FUa] Fung, Y.C., **Biomechanics**, Springer-Verlag, New York (1981).

[FUb] Fung, Y.C., **Biomechanics: Mechanical Properties of Living Tissues** Springer-Verlag, New York (1993).

[GEa] Geselowitz, D.B. and Miller, W.T., A bidomain model for anisotropic cardiac muscle, *Ann. Biomed. Eng.*, **11** (1983), 191–206.

[GIa] Giancotti, F.G. and Ruoslahti, E., Integrin signaling, *Science*, **285** (1999), 1028–1032.

[GLa] Gleason, R.L. and Humphrey, J.D., A mixture model of arterial growth and remodeling in hypertension: Altered muscle tone and tissue turnover, *J. Vasc. Res.*, **41** (2004), 352–363.

[GLb] Gleason, R.L. and Humphrey, J.D., Effects of a sustained extension on arterial growth and remodeling: A theoretical study, *J. Biomech.*, **38** (2005), 1255–1261.

[GLc] Glover, D.M., Gonzalez, C., and Raff, J.W., The centrosome, *Sci. Amer.*, **268** (1993), 62–68.

[GOa] Gohring, W., Sasaki, T., Heldin, C.H., and Timpl, R., Mapping of the binding of platelet-derived growth factor to distinct domains of the basement membrane proteins BM-40 and perlecan and distinction from the BM-40 collagen-binding epitope, *Eur. J. Biochem.*, **255** (1998), 60–66.

[HAa] Hayashi, K., Experimental approaches on measuring the mechanical properties and constitutive laws of arterial walls, *J. Biomech. Eng.*, **115** (1993), 481–488.

[HEa] He, C.M. and Roach, M.R., The composition and mechanical properties of abdominal aortic aneurysms, *J. Vasc. Surg.*, **20** (1994), 6–13.

[HEb] Heeschen, C., Lehmann, R., Honold, J., Assmus, B., Aicher, A., Walter, D.H., Martin, H., Zeiher, A.M., and Dimmeler, S., Profoundly reduced neovascularization capacity of bone marrow mononuclear cells derived from patients with chronic ischemic heart disease, *Circulation*, **109** (2004), 1615–1622.

[HEc] Heethaar, R.M, Pao, Y.C., and Ritman, E.L., Computer aspects of three-dimensional finite element analysis of stresses and strains in the intact heart, *Comput. Biomed. Res.*, **10** (1977), 271–285.

[HEd] Hénon, S., Lenormand, G., Richert, A., and Gallet, F., A new determination of the shear modulus of the human erythrocyte membrane using optical tweezers, *Biophys. J.*, **76** (1999), 1145–1151.

[HEe] Heusch, G., Post, H., Michel, M.C., Kelm, M., and Schulz, R., Endogenous nitric oxide and myocardial adaptation to ischemia, *Circ. Res.*, **87** (2000), 146–152.

[HIa] Hill, J.M., Zalos, G., Halcox, J.P.J., Schenke, W.H., Waclawiw, M.A., Quyyumi, A.A., and Finkel, T., Circulating endothelial progenitor cells, vascular function, and cardiovascular risk, *N. Engl. J. Med.* **348** (2003), 593–600.

[HOa] Hochmuth, R.M., Micropipette aspiration of living cells, *J. Biomech.*, **33** (2000), 15–22.

[HOb] Holzapfel, G.A. and Gasser, T.C., A new constitutive framework for arterial wall mechanics and a comparative study of material models, *J. Elasticity*, **61** (2000), 1–48.

[HSa] Hsu, E.W. and Henriquez, C.S., Myocardial fiber orientation mapping using reduced encoding diffusion tensor imaging, *J. Cardiovasc. Magn. Reson.*, **3** (2001), 339–347.

[HUa] Humphrey, J.D. and Rajagopal, K.R., A constrained mixture model for growth and remodeling of soft tissues, *Math. Model. Meth. Appl. Sci.*, **12** (2002), 407–430.

[HUb] Humphrey, J.D., Continuum biomechanics of soft biological tissues, *Proc. R. Soc. Lond. A*, **459** (2003), 3–46.

[HUc] Hunter, P.J., McCulloch, A.D., and ter Keurs, H.E., Modelling the mechanical properties of cardiac muscle, *Prog. Biophys. Mol. Biol.*, **69** (1998), 289–331.

[HUd] Huxley, A.F., Muscle structure and theories of contraction, *Prog. Biophys. Chem.*, **7** (1957), 255–318.

[HUe] Huyghe, J.M., Arts, T., and van Campen, D.H., Porous medium finite element model of the beating left ventricle. *Am. J. Physiol.*, **262** (1992), H1256-H1267.

[HYa] Hynes, R.O., Fibronectins, *Sci. Am.*, **254** (1986), 42–51.

[INa] Ingber, D.E., Madri, J.A., and Jamieson, J.D., Role of basal lamina in neoplastic disorganization of tissue architecture, *Proc. Natl. Acad. Sci. USA*, **78** (1981), 3901–3905.

[IRa] Irizarry, E., Newman, K.M., Gandhi, R.H., Nackman, G.B., Halpern, V., Wishner, S., Scholes, J.V., and Tilson, M.D., Demonstration of interstitial collagenase in abdominal aortic aneurysm disease, *J. Surg. Res.*, **54** (1993), 571–574.

[ITa] Ito, H., Hirata, Y., Hiroe, M., Tsujino, M., Adachi, S., Takamoto, T., Nitta, M., Taniguchi, K., and Marumo, F., Endothelin-1 induces hypertrophy with enhanced expression of muscle-specific genes in cultured neonatal rat cardiomyocytes, *Circ. Res.*, **69** (1991), 209–215.

[JEa] Jennings, L.M., Butterfield, M., Booth, C., Watterson K.G., and Fisher, J., The pulmonary bioprosthetic heart valve: its unsuitability for use as an aortic valve replacement. *J. Heart Valve Dis.*, **11** (2002), 668–678.

[JOa] Johnson, P.C., The myogenic response, In **Handbook of Physiology. The Cardiovascular System. Vascular Smooth Muscle**, sect. 2, vol. II, chapt. 15, Am. Physiol. Soc., Bethesda, MD, (1981), pp. 409–442.

[JOb] Joly, M., Lacombe, C., and Quemada, D., Application of the transient flow rheology to the study of abnormal human bloods, *Biorheology*, **18** (1981), 445–452.

[KAa] Katusic, Z.S., Superoxide anion and endothelial regulation of arterial tone, *Free Radic. Biol. Med.*, **20** (1996), 443–448.

[KEa] Keller, E.F. and Segel, L.A., Model for chemotaxis, *J. Theor. Biol.*, **30** (1971), 225–234.

[KEb] Kermorgant, S., Zicha, D., and Parker, P.J., PKC controls HGF-dependent c-Met traffic, signalling and cell migration, *EMBO J.*, **23** (2004), 3721–3734.

[KIa] Kirkham, M., Fujita, A., Chadda, R., Nixon, S.J., Kurzchalia, T.V., Sharma, D.K., Pagano, R.E., Hancock, J.F., Mayor, S., Parton, R.G., and Richards, A.A., Ultrastructural identification of uncoated caveolin-independent early endocytic vehicles, *J. Cell Biol.*, **168** (2005), 465–476.

[KUa] Kuharsky, A.L. and Fogelson, A.L., Surface-mediated control of blood coagulation: the role of binding site densities and platelet deposition, *Biophys. J.*, **80** (2001), 1050–1074.

[LAa] Laugwitz, K.L., Moretti, A., Lam, J., Gruber, P., Chen, Y., Woodard, S., Lin, L.Z., Cai, C.L., Lu, M.M., Reth, M., Platoshyn, O., Yuan, J.X., Evans, S., and Chien, K.R., Postnatal isl1+ cardioblasts enter fully differentiated cardiomyocyte lineages, *Nature*, **433** (2005), 647–653.

[LAb] Laurent, V., Planus, E., Isabey, D., Lacombe, C., and Bucherer, C., Propriétés mécaniques de cellules endothéliales évaluées par micromanipulation cellulaire et magnétocytométrie, **MecanoTransduction 2000**, Ribreau, C. et al. Eds., Tec&Doc, Paris (2000), pp. 373–380.

[LEa] Le, P.U. and Nabi, I.R., Distinct caveolae-mediated endocytic pathways target the Golgi apparatus and the endoplasmic reticulum, *J. Cell Sci.*, **116** (2003), 1059–1071.

[LEb] le Noble, F., Moyon, D., Pardanaud, L., Yuan, L., Djonov, V., Matthijsen, R., Breant, C., Fleury, V., and Eichmann, A., Flow regulates arterial-venous differentiation in the chick embryo yolk sac. *Development*, **131** (2004), 361–375.

[MAa] Manoussaki, D., A mechanochemical model of angiogenesis and vasculogenesis, *Math. Model. Numer. Anal.*, **37** (2003), 581–599.

[MAb] Marrocco, A., Numerical simulation of chemotactic bacteria aggregation via mixed finite elements, *Math. Model. Numer. Anal.*, **37** (2003), 617–630.

[MEa] Meili, R., Sasaki, A.T., and Firtel, R.A., Rho Rocks PTEN, *Nature Cell Biology*, **7** (2005), 334–335.

[MEb] Meininger, G.A. and Davis, M.J., Cellular mechanisms involved in the vascular myogenic response, *Am. J. Physiol., Heart Circ. Physiol.*, **263** (1992), H647–H659.

[MIa] Michel, C.C. and Curry, F.E., Microvascular permeability, *Physiol. Rev.*, **79** (1999), 703–761.

[MOa] Morawietz, H., Talanow, R., Szibor, M., Rueckschloss, U., Schubert, A., Bartling, B., Darmer, D., and Holtz, J., Regulation of the endothelin system by shear stress in human endothelial cells. *J. Physiol.*, **525** (2000), 761–770.

[MUa] Murray, C.D., The physiological principle of minimum work. I. The vascular system and the cost of blood volume, *Proc. Nat. Acad. Sci.* (USA), **12** (1926), 207–214.

[MUb] Murray, J., Osher, G., and Harris, A., A mechanical model for mesenchymal morphogenesis, *J. Math. Biol.*, **17** (1983), 125–129.

[MUc] Murray, J.D., **Mathematical Biology**, Springer-Verlag, New York (2002).

[NAa] Nagumo, J., Arimoto, S., and Yoshizawa, S., An active pulse transmission line simulating nerve axons, *Proc. IRE*, **50** (1962), 2061–2070.

[NOa] Nobes, C.D. and Hall, A., Rho, rac, and cdc42 GTPases regulate the assembly of multimolecular focal complexes associated with actin stress fibers, lamellipodia, and filopodia. *Cell*, **81** (1995), 53–62.

[NOb] Nollert, M.U., Eskin, S.G., and McIntire, L.V., Shear stress increases inositol trisphosphate levels in human endothelial cells, *Biochem. Biophys. Res. Commun.*, **170** (1990), 281–287.

[NOc] Nollert, M.U., Diamond, S.L., and McIntire, L.V., Hydrodynamic shear stress and mass transport modulation of endothelial cell metabolism, *Biotechnol. Bioeng.*, **38** (1991), 588–602.

[ODa] Oddou, C. and Ohayon, J., Mécanique de la structure cardiaque, In **Biomécanique des fluides et des tissus**, Jaffrin, M.Y., and Goubel, F. Eds., Masson, Paris (1998), pp. 247–292.

[OZa] Ozdamar, B., Bose, R., Barrios-Rodiles, M., Wang, H.R., Zhang, Y., and Wrana, J.L., Regulation of the polarity protein Par6 by TGF-beta receptors controls epithelial cell plasticity. *Science*, **307** (2005), 1603–1609.

[PAa] Pavalko, F.M. and Otey, C.A., Role of adhesion molecule cytoplasmic domains in mediating interactions with the cytoskeleton, *Proc. Soc. Exp. Biol. Med.*, **205** (1994), 282–293.

[PEa] Peskin, C.S., Fiber architecture of the left ventricular wall: An asymptotic analysis, *Commun. Pure Appl. Math.*, **42** (1989), 79–113.

[PEb] Peskin, C.S. and McQueen, D.M., Mechanical equilibrium determines the fractal fiber architecture of aortic heart valve leaflets, *Am. J. Physiol.*, **266** (1994), H319-H328.

[PIa] Pieske, B., Beyermann, B., Breu, V., Loffler, B.M., Schlotthauer, K., Maier, L.S., Schmidt-Schweda, S., Just, H., and Hasenfuss, G., Functional effects of endothelin and regulation of endothelin receptors in isolated human nonfailing and failing myocardium, *Circulation*, **99** (1999), 1802–1809.

[PIb] Pioletti, D.P. and Rakotomanana, L.R., Non-linear viscoelastic laws for soft biological tissues, *Eur. J. Mech. A/Solids*, **19** (2000), 749–759.

[POa] Pohl, U. and Busse, R., Hypoxia stimulates release of endothelium-derived relaxant factor, *Am. J. Physiol.*, **256** (1989), H1595–H1600.

[POb] Poon, C.S. and Merrill, C.K., Decrease of cardiac chaos in congestive heart failure, *Nature*, **389** (1997), 492–495.

[RAa] Rabiet, M.J., Plantier, J.L., Rival, Y., Genoux, Y., Lampugnani, M.G., and Dejana, E., Thrombin-induced increase in endothelial permeability is associated with changes in cell-to-cell junction organization, *Arterioscler. Thromb. Vasc. Biol.*, **16** (1996), 488–496.

[RAb] Raghavan, M.L., Vorp, D.A., Federle, M.P., Makaroun, M.S., and Webster, M.W., Wall stress distribution on three-dimensionally reconstructed models of human abdominal aortic aneurysm, *J. Vascular Surgery*, **31** (2000), 760–769.

[RAc] Rajagopal, K.R. and Srinivasa, A.R., A thermodynamic framework for rate-type fluid models, *J. Non-Newtonian Fluid Mech.*, **88** (2000), 207–227.

[RAd] Raval, A.P., Dave, K.R., Prado, R., Katz, L.M., Busto, R., Sick, T.J., Ginsberg, M.D., Mochly-Rosen, D., and Perez-Pinzon, M.A., Protein kinase C delta cleavage initiates an aberrant signal transduction pathway after cardiac arrest and oxygen glucose deprivation, *J. Cereb. Blood Flow Metab.*, **25** (2005), 730–741.

[RAe] Rayment, I., Holden, H.M., Whittaker, M., Yohn, C.B., Lorenz, M., Holmes, K.C., and Milligan, R.A., Structure of the actin-myosin complex and its implications for muscle contraction, *Science*, **261** (1993), 58–65.

[ROa] Robert, L., Elasticité des tissus et vieillissement, *Pour la science*, **201** (1994), 56–62.

[ROb] Robinson, T.F., Factor, S.M., and Sonnenblick, E.H., The heart as a suction pump, *Sci. Amer.*, **6** (1986), 62–69.

[SAa] Sainte-Marie, J., Chapelle, D., and Sorine, M., Data assimilation for an electro-mechanical model of the myocardium, In **Second M.I.T.**

Conference on Computational Fluid and Solid Mechanics, Bathe, K.J. Ed. (2003), pp. 1801–1804.

[SAb] Sata, M., Saiura, A., Kunisato, A., Tojo, A., Okada, S., Tokuhisa, T., Hirai, H., Makuuchi, M., Hirata, Y., and Nagai, R., Hematopoietic stem cells differentiate into vascular cells that participate in the pathogenesis of atherosclerosis, *Nat. Med.*, **8** (2002), 403–409.

[SAc] Sato, M., Theret, D.P., Wheeler, L.T., Ohshima, N., and Nerem, R.M., Application of the micropipette technique to the measurement of cultured porcine aortic endothelial cells viscoelastic properties, *Trans. ASME J. Biomech. Eng.*, **112** (1990), 263–268.

[SCa] Schaller, M.D. and Parsons, J.T., pp125FAK-dependent tyrosine phosphorylation of paxillin creates a high-affinity binding site for Crk, *Mol. Cell. Biol.*, **15** (1995), 2635–2645.

[SCb] Schenkel, A.R., Mamdouh, Z., and Muller W.A., Locomotion of monocytes on endothelium is a critical step during extravasation, *Nature Immunology*, **5** (2004), 393–400.

[SCc] Schmidt, F.G., Hinner, B., Sackmann, E., and Tang, J.X., Viscoelastic properties of semiflexible filamentous bacteriophage fd, *Phys. Rev. E Stat. Phys. Plasmas Fluids Relat. Interdiscip. Topics*, **62** (2000), 5509–5517.

[SEa] Sermesant, M., Forest, C., Pennec, X., Delingette, H., and Ayache, N., Deformable biomechanical models: application to 4D cardiac image analysis, *Med. Image. Anal.*, **7** (2003), 475–488.

[SHa] Sheng, M., McFadden, G., and Greenberg, M.E., Membrane depolarization and calcium induce c-fos transcription via phosphorylation of transcription factor CREB, *Neuron*, **4** (1990), 571–82.

[SIa] Sipido, K.R., Callewaert, G., and Carmeliet, E., Inhibition and rapid recovery of Ca2+ current during Ca2+ release from sarcoplasmic reticulum in guinea pig ventricular myocytes, *Circ. Res.*, **76** (1995), 102–109.

[SMa] Smith, N.P., Pullan, A.J., and Hunter, P.J., An anatomically based model of transient coronary blood flow in the heart, *SIAM J. Appl. Math.*, **62** (2002), 990–1018.

[SMb] Smyth, S.S., Joneckis, C.C., and Parise L.V., Regulation of vascular integrins, *Blood*, **81** (1993), 2827–2843.

[SOa] Sobolewski, K., Wolanska, M., Bankowski, E., Gacko, M., and Glowinski, S., Collagen, elastin and glycosaminoglycans in aortic aneurysms, *Acta Biochim. Pol.*, **42** (1995), 301–307.

[STa] Steinman, D.A., Milner, J.S., Norley, C.J., Lownie, S.P., and Holdsworth, D.W., Image-based computational simulation of flow

dynamics in a giant intracranial aneurysm, *Am. J. Neuroradiol.*, **24** (2003), 559–566.

[STb] Stergiopulos, N., Tardy, Y., and Meister, J.J., Nonlinear separation of forward and backward running waves in elastic conduits, *J. Biomech.*, **26** (1993), 201–209.

[STc] Stergiopulos, N., Westerhof, B.E., and Westerhof, N., Total arterial inertance as the fourth element of the windkessel model *Am. J. Physiol., Heart Circ. Physiol.*, **276** (1999), H81–H88.

[STd] Stradins, P., Lacis, R., Ozolanta, I., Purina, B., Ose, V., Feldmane, L., and Kasyanov, V., Comparison of biomechanical and structural properties between human aortic and pulmonary valve, *Eur. J. Cardiothorac. Surg.*, **26** (2004), 634–639.

[SUa] Surks, H.K., Mochizuki, N., Kasai, Y., Georgescu, S.P., Tang, K.M., Ito, M., Lincoln, T.M., and Mendelsohn, M.E., Regulation of myosin phosphatase by a specific interaction with cGMP-dependent protein kinase Iα, *Science*, **286** (1999), 1583–1587.

[THa] Theret, D.P., Levesque, M.J., Sato, M., Nerem, R.M., and Wheeler, L.T., The application of a homogeneous half-space model in the analysis of endothelial cell micropipette measurements, *Trans. ASME J. Biomech. Eng.*, **110** (1988), 190–199.

[THb] Thiriet, M., Issa, R., and Graham, J.M.R., A pulsatile developing flow in a bend, *J. Phys. III* (1992), 995–1013.

[THc] Thiriet, M., Pares, C., Saltel, E., and Hecht, F., Numerical model of steady flow in a model of the aortic bifurcation, *ASME J. Biomech. Eng.*, 114 (1992), 40–49.

[THd] Thiriet, M., Martin-Borret G., and Hecht, F., Ecoulement rhéofluidifiant dans un coude et une bifurcation plane symétrique. Application à l'écoulement sanguin dans la grande circulation, *J. Phys. III*, **6** (1996), 529–542.

[TUa] Tunggal, J.A., Helfrich, I., Schmitz, A., Schwarz, H., Ganzel, D., Fromm, M., Kemler, R., Krieg, T., and Niessen, C.M., E-cadherin is essential for in vivo epidermal barrier function by regulating tight junctions, *EMBO J.*, **24** (2005), 1146–1156.

[TUb] Turner, C.E., Paxillin and focal adhesion signalling, *Nat. Cell Biol.*, **2** (2000), E231–236.

[VAa] van Nieuw Amerongen G.P. and van Hinsbergh, V.W.M., Cytoskeletal effects of Rho-like small guanine nucleotide-binding proteins in the vascular system, *Arterioscler. Thromb. Vasc. Biol.*, **21** (2001), 300–311.

[VAb] van Royen, N., Piek, J.J., Buschmann, I., Hoefer, I., Voskuil, M., and Schaper, W., Stimulation of arteriogenesis: a new concept for the

treatment of arterial occlusive disease, *Cardiovasc. Res.*, **49** (2001), 543–553.

[VAc] Vanhoutte, P.M., Endothelial dysfunction and atherosclerosis, *Eur. Heart J.*, **18** (1997), E19–29.

[VEa] Verdier, C., Rheological properties of living materials : from cells to tissues, *J. Theor. Med.*, **5** (2003), 67–91.

[VEb] Veronda, D.R. and Westmann, R.A., Mechanical characterization of skin. Finite deformation, *J. Biomech.*, **3** (1970), 114–124.

[VIa] Viidik, A., Properties of tendons and ligaments, In **Handbook of Bioengineering**, Skalak, R., and Chien, S. Eds., McGraw-Hill, New York (1987), 6.1–6.19.

[VIb] Villarreal, F.J., Lew, W.Y., Waldman, L.K., and Covell, J.W., Transmural myocardial deformation in the ischemic canine left ventricle, *Circ. Res.*, **68** (1991), 368–381.

[WAa] Wagner, D.D., The Weibel-Palade body: The storage granule for von Willebrand factor and P-selectin, *Thromb. Haemost.* **70** (1993), 105–110.

[WAb] Wang, N., Butler, J.P., and Ingber, D.E., Mechanotransduction across the cell surface and through the cytoskeleton, *Science*, **260** (1993), 1124–1127.

[WEa] Weinbaum, S. and Curry, F.E., Modelling the structural pathways for transcapillary exchange *Symp. Soc. Exp. Biol.*, **49** (1995), 323–345.

[WEb] Westerhof, N., Bosman, F., De Vries, C.J., and Noordergraaf, A., Analog studies of the human systemic arterial tree, *J. Biomechanics*, **2** (1969), 121–143.

[WUa] Wu, J.Z. and Herzog, W., Modelling concentric contraction of muscle using an improved cross-bridge model, *J. Biomech.*, **32** (1999), 837–848.

[YAa] Yang, M., Taber, L.A., and Clark, E.B., A nonliner poroelastic model for the trabecular embryonic heart, *J. Biomech. Eng.*, **116** (1994), 213–223.

[YAb] Yap, A.S., Brieher, W.M., and Gumbiner, B.M., Molecular and functional analysis of cadherin-based adherens junctions, *Annu. Rev. Cell. Dev. Biol.*, **13** (1997), 119–146.

[YEa] Yeung, A. and Evans, E., Cortical shell-liquid core model for passive flow of liquid-like spherical cells into micropipets, *Biophys. J.*, **56** (1989), 139–149.

[YUa] Yurchenco, P.D. and O'Rear, J.J., Basal lamina assembly, *Curr. Opin. Cell Biol.*, **6** (1994), 674–681.

[ZAa] Zahalak, G.I., A distribution-moment approximation for kinetic theories of muscular contraction, *Math. Biosci.*, **114** (1981), 55–89.

[ZAb] Zamir, E. and Geiger, B. Components of cell-matrix adhesions, *J. Cell Sci.*, **114** (2001), 3577–3579.

[ZIa] Zimmermann, S., and Moelling, K., Phosphorylation and regulation of Raf by Akt (protein kinase B). *Science*, **286** (1999), 1741–1744.

[ZUa] Zühlke, R.D., Pitt, G.S., Deisseroth, K., Tsien, R.W., and Reuter, H., Calmodulin supports both inactivation and facilitation of L-type calcium channels, *Nature*, **399** (1999), 159–162.

[ZUb] Zulliger, M.A., Rachev, A., and Stergiopulos, N., A constitutive formulation of arterial mechanics including vascular smooth muscle tone, *Am. J. Physiol. Heart Circ. Physiol.*, **287** (2004), H1335–H1343.